# MPK3 and MPK6 control salicylic acid signaling by up-regulating NLR receptors during pattern- and effector-triggered immunity

Julien Lang, Baptiste Genot, Jean Bigeard, Jean Colcombet

# MAP Kinases 3 and 6 control Salicylic Acid signaling by upregulating *NLR* receptors during Pattern- and Effector-Triggered Immunity.

**Running title: MPK3/6 bridge PTI and ETI through *NLR* expression**

Julien Lang[1,2], Baptiste Genot[1,2,3], Jean Bigeard[1,2] and Jean Colcombet[1,2]

[1] Institute of Plant Sciences Paris Saclay (IPS2), CNRS, INRAE, UEVE, Université Paris-Saclay, 91405 Orsay, France

[2] Institute of Plant Sciences Paris Saclay (IPS2), CNRS, INRAE, UEVE, Université de Paris, 91405 Orsay, France

[3] Present address: Bigelow Laboratory for Ocean Sciences, East Boothbay, ME, United States

Email addresses: julien.lang@inrae (JL), bgenot@bigelow.org (BG), jean.bigeard@univ-evry.fr (JB), jean.colcombet@inrae.fr (JC)

For correspondance: julien.lang@inrae.fr

Key words: MAPK signaling, ETI, PTI, *Arabidopsis thaliana*, plant immunity

## Highlight

Upregulation of *NLR* immune receptor genes is common to PTI and ETI, relies on similar, albeit differently articulated, PTI and ETI signaling components, and promotes the SA sector of defense.


## Abstract

*Arabidopsis thaliana* Mitogen-Activated Protein Kinases 3 and 6 (MPK3/6) are transiently activated during PAMP-Triggered Immunity (PTI) and durably during Effector-Triggered Immunity (ETI). However the functional differences between these two kinds of activation kinetics and how they coordinate the two layers of plant immunity remain poorly understood. Here, by suppressor analyses, we demonstrate that ETI-mediating Nucleotide-binding domain Leucine-rich repeat Receptors (NLRs) and the NLR signaling components NDR1 and EDS1 can promote the SA sector of defense downstream of MPK3 activity. Moreover we provide evidence that both sustained and transient MPK3/6 activities positively control the expression of several *NLR* genes, including *AT3G04220* and *AT4G11170*. We further show that NDR1 and EDS1 also contribute to the upregulations of these two *NLRs* not only in an ETI context but also in a PTI context. Remarkably, while in ETI, MPK3/6 activities are dependent on NDR1 and EDS1, they are not in PTI, suggesting crucial differences in the two signaling pathways. Finally we demonstrate that expression of the *NLR AT3G04220* is sufficient to induce expression of defense genes from the SA branch. Overall this study enlarges our knowledge of MPK3/6 functions during immunity and gives a new insight into the intrication of PTI and ETI.



## Keywords

Mitogen-Activated Protein Kinase (MAPK), MPK3/6, *Arabidopsis thaliana*, plant immunity, PTI, ETI, *Pseudomonas syringae*, Salicylic Acid (SA), defense signaling

## Introduction

The plant defense responses to pathogens are usually viewed as a two-layered system (Jones and Dangl, 2006). In the first one, cell surface-localized Pattern-Recognition Receptors (PRRs) recognize conserved Pathogen-Associated Molecular Patterns (PAMPs), thereupon eliciting PAMP-Triggered Immunity (PTI). The family of PRRs comprises Leucine-Rich Repeat (LRR) Receptor Kinases (LRR-RKs) and LRR Receptor Proteins (LRR-RPs) which differ in their mechanisms of signal transduction but are supposed to converge towards conserved PTI responses (Zipfel, 2014). In the second layer of immunity, pathogen effectors, secreted to counteract plant defense responses and to favor plant susceptibility, are recognized by intracellular Nucleotide-binding domain LRR Receptors (NLRs) giving rise to the Effector-Triggered Immunity (ETI) (Cui et al., 2015). Although signaling events involved in PTI are relatively well known including Receptor-Like Cytoplasmic Kinases (RLCKs), Mitogen-Activated Protein Kinases (MAPKs), Calcium-Dependent Protein Kinases (CDPKs) and ROS (Bigeard et al., 2015), the signaling mechanisms of ETI, on the other hand, remain more elusive. The existence of two main classes of NLRs, containing in their N-terminal part either a Coiled-Coil (CC) domain for CC-NLR (CNL) or a Toll and Interleukin-1 Receptor (TIR) domain for TIR-NLR (TNL), suggests that ETI signaling might be processed through two distinct pathways depending on the type of NLR involved. For instance initial reports supported the notion that Non-race specific Disease resistance 1 (NDR1) mediates CNL-ETI while Enhanced Disease Susceptibility 1 (EDS1) contributes to TNL-ETI (Aarts et al., 1998). However further studies undermined this conception, by revealing that CNL-ETI could be independent of NDR1 (Day et al., 2006; Kapos et al., 2019), that EDS1 could play a role in CNL-ETI (Bhandari et al., 2019; Venugopal et al., 2009), and that CNLs and TNLs could cooperate (Wu et al., 2019).

In addition to this, the strict dichotomy between PTI and ETI that would be consecutive in time and would each represent a specific kind of immunity, has been regularly challenged. Studies showing that PTI and ETI not only share numerous signaling components but also lead to similar gene reprogramming progressively built a model in which PTI and ETI are continuously linked, with connections allowing sophisticated and extensive modulations of plant defense responses (Lu and Tsuda, 2020; Peng et al., 2018; Tsuda and Katagiri, 2010; Yuan et al., 2021b). For instance, using a combination of mutants in key defense genes, it

was shown that the *Arabidopsis* immune network is composed of four main sectors – the three phytohormone jasmonate, ethylene and salicylic acid (SA) sectors plus the lipase-like Phytoalexin Deficient 4 sector -, and that these four sectors are essential for both PTI- and ETI, although they are differently articulated in the two contexts, enabling synergistic effects during PTI and rather robust responses during ETI (Tsuda et al., 2009). More recently it has also been uncovered that PTI responses are required for optimization of ETI responses and that in return ETI responses promote accumulation of PTI actors, demonstrating thereby a mutal potentiation of the two kinds of immunity (Ngou et al., 2021; Yuan et al., 2021a). Despite these significant advances, the question of the molecular mechanisms underlying the crosstalks between PTI and ETI remains one of the most exciting in the field of plant-microbe interactions (Harris et al., 2020).

MAPKs are essential signaling components that allow plants to integrate various cues coming from biotic and abiotic stresses or developmental programs, into appropriate cell responses (Colcombet and Hirt, 2008). A canonical MAPK cascade encompasses a MAPK Kinase Kinase (MAP3K), a MAPK Kinase (MAP2K or MKK) and a MAPK (or MPK) which activate in a serial manner by phosphorylation (Ichimura et al., 2002). Active MAPKs can subsequently phosphorylate specific substrates on specific sites, thereby translating signal inputs into functional outputs (Dóczi and Bögre, 2018). In the context of immunity, two MAPK cascades have been particularly well characterized. The rapid and transient activation of both MAP3K3/5-MKK4/5-MPK3/6 and MEKK1-MKK1/2-MPK4 cascades, upon PAMP perception, leads to a gene reprogramming that is instrumental in mounting succesful PTI responses (Asai et al., 2002; Frei dit Frey et al., 2014; Gao et al., 2008; Sun et al., 2018). Recently it has been shown that MPK3/6 could also be activated in a sustained manner in response to effector recognition, and several roles, such as buffering of the SA sector of defense, promotion of camalexin production, or inhibition of the photosystem have been associated with this phenomenon (Su et al., 2018; Tsuda et al., 2013; Xu et al., 2016). Nonetheless it is not clear so far whether these functions are specific of sustained MPK3/6 activations or the simple extension of processes already controlled by transient MPK3/6 activations. Similarly the question whether sustained MPK3/6 activations constitute a general feature of ETI or are restricted to peculiar effector/NLR recognitions remains debatable (Lang and Colcombet, 2020).

Here, starting with an analysis of the regulation and functions of sustained MPK3/6 activations during ETI, we came to the finding that MPK3/6 activities could bridge PTI and ETI by positively controlling the SA sector of defense through the expression of some *NLR* genes. We also showed that ETI-regulating NDR1 and EDS1 are involved in this process. Altogether our results unveil an original intrication between PTI and ETI components.

## Materials and Methods

### Plasmid constructs

The *AT3G04220* coding sequence was amplified from *Arabidopsis* cDNA using the primers CACCATGGATTCTTCTTTTTTAC and GCATTTATAAAACTTCAATCTCTTG. Sequencing revealed a 27 bp insertion after nucleotide 1935 comparatively to the reference sequence from TAIR10. This new sequence was then introduced by digestion/ligation between the XhoI and StuI restriction sites in a dexamethasone-inducible expression vector (X. Gao et al., 2013).

### Plant materials and growth conditions

All plants from this study are in the Columbia background. The *rps2rpm1* (Nobori et al., 2018), *rps4-2* (Saucet et al., 2015), *eds1-2* (Bartsch et al., 2006), *ndr1-1* (Century et al., 1995), *mpk3-1* (Zhao et al., 2014), *mpk6-4* (Xu et al., 2008), *mkk4-18/mkk5-18* (Li et al., 2018), and K3CA-2 and K3WT-1 (Genot et al., 2017) backgrounds were described previously. The *snc1-11* (SALK_116460), *at4g11170* (SALK_007034) and *at3g04220* (GABI_290D03) lines were purchased from the NASC and homozygous plants were selected by genotyping using LBb1.3 (SALK), o849 (GABI), TGGTGATTCCGATTTTCTTCCAC and TCTGTTGCTTTAACCTTTGCTCC (*snc1-11*), TTTAGCGGTCAACACGAAAAC and CCAAAATTGAAAATAGAGAACCC (*at4g11170*), and GTCGTCTTTATCTCTCACGCG and GAAGGGCCTCTTCATAGTTGG (*at3g04220*) primers. The DEX-*AT3G04220*/*at3g04220* line was obtained by floral dip, and transformed plants were selected on hygromycin. The K3CA-2/*ndr1-1*, K3CA-2/*eds1-2* and K3CA-2/*snc1-11* lines were obtained by crosses and homozygous plants were selected by genotyping and segregation analysis.

All plants were grown in growth rooms at 20°C in short day conditions (8 h light / 16 h dark) at 60 % hygrometry and under a light intensity of approximatively 150 µmol $m^{-2}$ $s^{-1}$.

## Plant treatments and bacterial infections

All treatments (chemical and bacterial infections) were performed on 1.5 month-old plants by syringe infiltration. The PAMP flg22 and the steroids estradiol and dexamethasone were used at 1 µM, 10 µM and 5 µM respectively in 10 mM $MgCl_2$. The *Pseudomonas syringae* pv. *tomato* DC3000 WT, AvrRpt2, AvrRpm1, AvrRps4 (Aarts et al., 1998) and the non-polar *hrcC-* (Peñaloza-Vázquez et al., 2000) strains were described previously. The bacteria were grown on solid NYGA medium (0.5 % bactopeptone, 0.3 % yeast extract, 2 % glycerol, 1.5 % agar) and liquid LB medium supplemented with the appropriate antibiotics (50 µg/ml rifampycin for WT and *hrcC-*, and 50 µg/ml rifampycin + 25 µg/ml kanamycin for AvrRpt2, AvrRpm1 and AvrRps4).

Fresh cultures of bacteria were washed and resuspended in 10 mM $MgCl_2$ at a final $OD_{600}$=0.015 for RNA and protein analyses, and at a final $OD_{600}$=0.005 for pathoassays. Technical repeats were typically constituted from punches of leaves coming from at least 2 different plants. Bacteria load was quantified by counting the colony forming units.

## Protein Methods

For immunoblotting, proteins were extracted in a nondenaturant buffer (50 mM Tris-HCl pH 7.5, 150 mM NaCl, 0.1 % NP40, 5 mM EGTA, 0.1 mM DTT) or in nondenaturant Laccus buffer (15 mM EGTA, 15 mM $MgCl_2$, 75 mM NaCl, 1 % Tween, 25 mM Tris-HCl pH 7.5, 1 mM DTT) in presence of inhibitors of proteases and phosphatases, and then quantified by Bradford assay. About 10 µg of total proteins were loaded on SDS-PAGE gels. The antibodies used were anti-pTpY (Cell Signaling 4370L), anti-MPK3 (Sigma M8318), anti-MPK6 (Sigma A7104), anti-H3 (Abcam Ab1791), and anti-PEPC (ThermoFischer 4100-4163) at 1/10 000 dilution.

For immunoprecipitation, proteins were extracted in a Laccus nondenaturant buffer in presence of inhibitors of proteases and phosphatases, and then quantified by Bradford assay. 100 µg of total proteins were mixed with 20 µl of sepharose beads (GE Healthcare) and 0.5 µl of anti-myc (Sigma C3956) antibody and incubated for 2 h with gentle shaking at 4°C. Then the immunoprecipitates were washed 2 times in SUC1 buffer (50 mM Tris-HCl pH

7.4, 250 mM NaCl, 5 mM EGTA, 5 mM EDTA, 0.1 % Tween) and 2 times in Kinase buffer (20 mM Hepes pH 7.5, 15 mM $MgCl_2$, 5 mM EGTA, 1 mM DTT).

For kinase assays, immunoprecipitates were resuspended in 15µl of kinase buffer containing 0.1 mM ATP, 1 $mg.ml^{-1}$ MBP and 2 µCi ATP [γ-33P]. After 30 min of reaction at room temperature samples were loaded on SDS-PAGE gel. Then the gels were dried and revealed using an Amersham™ Typhoon™ imager.

For nucleocytoplasmic fractioning, proteins were extracted in Honda buffer (2.5 % Ficoll type 400, 5 % Dextran MW 35-45 k, 0.4 M sucrose, 25 mM Tris-HCl pH 7.5, 10 mM $MgCl_2$, 5 mM DTT) in presence of inhibitors of proteases and phosphatases. After 15 min of incubation on ice in presence of 0.5 % Triton X-100, an aliquot corresponding to the total fraction was collected. After centrifugation at 1500 g for 5 min at 4°C, an aliquot of the supernatant corresponding to the nuclei-depleted fraction was collected. After washing with Honda buffer + 0.1 % Triton X-100, the pellet was resuspended in Honda buffer and this sample corresponded to the nuclei-enriched fraction.

**RNA Methods**

RNA was extracted using Nucleospin™ RNA Plus Kit (Macherey Nagel) according to the manufacturer's instructions and quantified with a Nanodrop spectrophotometer. Typically 1 µg of total RNA was used to perform RT reaction, using SuperScript™ II Reverse Transcriptase (Invitrogen) and following manufacturer's instructions. Quantitative PCRs were carried out with a LightCycler® 480 System (96 wells), using LightCycler® 480 SYBR Green I Master (Roche), and following the manufacturer's standard instructions. *ACT2* (*AT3G18780*) was used as an internal reference to calculate relative expression. Occasionally *SAND* (*AT2G28390*) was used as an internal reference to verify that the results were not biased by the choice of *ACT2*. The primers used for qPCR are listed in Table S1.

**Results**

**Sustained MAPK activation is characteristic of RPS2/RPM1-mediated ETI responses, concerns mostly MPK3 and leads to a nuclear accumulation of MPK3**

Sustained MPK3/6 activities have been reported in response to pathogen effectors (Su et al., 2018; Tsuda et al., 2013; Wang et al., 2018). Yet whether these activations represent a general feature of ETI remains controversial (Cui et al., 2017; Lang and Colcombet, 2020; Ngou et al., 2020). To get a better understanding of the question, we compared the pattern of MPK3/6 activities at late timepoints (5 hpi and 8 hpi), in Col-0 plants and after infiltration with mock or various *Pseudomonas syringae* pv. *tomato* DC3000 strains (referred hereafter as *Pst*), differing in their ability to stimulate plant immunity. The *Pst* WT strain expresses dozens of effectors but does not elicit a strong ETI response contrary to the *Pst* AvrRpt2, AvrRpm1 and AvrRps4 strains which express the eponymous effectors, while the *Pst hrcC*- strain is impaired in the effector translocation machinery and triggers only PTI responses. As shown in Figure 1A, MPK3/6 activities were the highest in response to *Pst* AvrRpt2 and AvrRpm1. We also observed a sustained activation in response to *Pst* AvrRps4 but which was significantly weaker than the previous ones. Finally the samples infiltrated with *Pst* WT and *hrcC*- did not reveal an activation signal different from the mock-treated samples. Furthermore we noticed that sustained MAPK activation concerned mostly MPK3 compared to MPK6 (Fig. 1A). Besides sustained MPK3 activation was correlated with a concomitant increase in the amount of MPK3 proteins whereas amounts of MPK6 remained globally unchanged (Fig 1A). However this MPK3 accumulation was not sufficient to explain the increase in activation which was of quite higher amplitude.

To confirm that the observed effects were really due to the recognition of the effectors, we compared the Col-0, *rps2rpm1* and *rps4-2* backgrounds. The CNLs RPS2 and RPM1 guard the RPM1-interacting protein 4 (RIN4) against modifications caused by AvrRpt2 and AvrRpm1 respectively (Belkhadir et al., 2004), while RPS4 contributes to the recognition of AvrRps4 (Saucet et al., 2015). Results indicated that both the MPK3/6 activations and the MPK3 accumulation were lost in *rps2rpm1* in response to *Pst* AvrRpt2 and AvrRpm1 (Fig. 1B). In contrast no clear differences could be detected between Col-0 and *rps4-2* in response to *Pst* AvrRps4 (Fig. S1), suggesting that the sustained MPK3/6 activation and MPK3 accumulation caused by this effector depends on other or additional receptors.

To determine whether sustained MPK3 activity and accumulation could affect its subcellular localization, we also quantified MPK3 protein abundance in nuclear and cytoplasmic fractions. The results of Figure 1C show that both fractions contain more MPK3 in response to *Pst* AvrRpt2 infiltration than in response to mock infiltration, although the abundance of MPK3 is very low in the nuclear fraction comparatively to the cytoplasmic fraction. Moreover the nuclear fraction is considerably more enriched (more than 10 times) than the cytoplasmic fraction (about 2 times), clearly indicating that in response to *Pst* AvrRpt2, MPK3 accumulates in the nucleus.

**NDR1 and EDS1 contribute to sustained but not transient MAPK activation**.

Both NDR1 and EDS1 are involved in the ETI signaling caused by AvrRpt2 recognition (Aarts et al., 1998; Bhandari et al., 2019; Day et al., 2006; Venugopal et al., 2009). To determine whether there is a link between these two regulators and sustained MPK3/6 activities, we measured the latters in the *ndr1-1* and *eds1-2* backgrounds. As shown in Figure 2A, there is a significant decrease in MPK3/6 activities in the two mutants, demonstrating that NDR1 and EDS1 act upstream of the MAPKs and contribute to their activation. Since we observed a concomitant decrease in the MPK3 protein level, we quantified normalized blot signals from independent experiments and concluded that the decrease in MPK3 activation in the two backgrounds is not due to the lower protein abundance, and also that the contribution of NDR1 to MPK3 activation is higher than that of EDS1 (Fig. 2B). Moreover, through nucleocytoplasmic fractioning, we found that the AvrRpt2-mediated nuclear enrichment of MPK3 was impaired in *ndr1-1* and *eds1-2* (Fig. 2C, 2D).

To consolidate the roles of NDR1 and EDS1 upstream of sustained MPK3/6 activities, we crossed the *ndr1-1* and *eds1-2* lines with the XVE-AvrRpt2 line that allows direct expression of the AvrRpt2 effector in the plant cell through an estradiol-inducible system (Tsuda et al., 2013) (Fig. S2), and again we could show that sustained MPK3/6 activities elicited by expression of AvrRpt2 are significantly compromised in absence of functional NDR1 and EDS1, with a higher contribution of NDR1 compared to EDS1 (Fig. 2E). .

Since NDR1 and EDS1 are instrumental in the sustained activation of MPK3/6, we were curious to see whether they also contribute to the transient activation of MPK3/6. To test this we infiltrated Col-0, *ndr1-1* and *eds1-2* leaves with the PAMP flg22 and quantified MPK3/6 activities at early timepoints. However, in this experimental set-up, we could not detect any significant difference between the three genotypes (Fig. 2F). As prior to this we made sure that mock-treated plants do not display PAMP-unrelated MAPK activation (Fig. S3), our results demonstrate that NDR1 and EDS1 are not involved in transient flg22-mediated MPK3/6 activations.

**Disturbed MAPK activities result in resistance/susceptibility phenotypes.**

In an attempt to understand the impact of sustained MPK3/6 activities on the plant defense responses and on the plant resistance to pathogens, we performed pathoassays with *Pst* AvrRpt2 in different plant backgrounds displaying modifications in the patterns of MPK3/6 activations. The K3CA-2 line is a gain-of-function line that expresses a mutated form of MPK3 under the control of the endogenous promoter. This line exhibits a higher basal level of MPK3 activity (Genot et al., 2017; Lang et al., 2017) and also a stronger sustained MPK3 activation upon *Pst* AvrRpt2 infiltration compared to a K3WT-1 line expressing a WT form of MPK3 (Fig. S4A). The single mutants *mpk3-1* and *mpk6-4* are defective in the respective MAPKs (Xu et al., 2008; Zhao et al., 2014), yet measurements of their sustained activities upon AvrRpt2 recognition revealed mild effects. As sustained MPK6 activation is weak in response to *Pst* AvrRpt2, the *mpk6-4* loss of function shows the strong MPK3 activation roughly unchanged, while in *mpk3-1*, we observed a drastic increase in the levels of MPK6 activations which somehow should compensate for the absence of MPK3 (Fig. S4B). At last the recently characterized *mkk4-18/mkk5-18* line (referred hereafter as *mkk4mkk5*) (Li et al., 2018) harbours a weak allele of MKK4 and a loss-of-function allele of MKK5, two genes coding for the MAP2Ks acting upstream of MPK3/6. Consistently the *mkk4mkk5* line shows a lower level of MPK3/6 activation both in response to *Pst* AvrRpt2 and flg22 (Fig. S4C, S4D).

In line with their patterns of MAPK activation, the K3CA-2 line appears more resistant to *Pst* AvrRpt2 infiltration than WT controls, whereas the *mkk4mkk5* line is more sensitive than the Col-0, even though it is not as sensitive as the *ndr1-1* line (Fig. 3). In addition we observed

that the *mpk3-1* (but not *mpk6-4*) and *eds1-2* lines behave in an intermediate fashion between Col-0 and *mkk4mkk5* (Fig. 3).

Overall our data demonstrate that MPK3/6 activities are important for resistance phenotypes. They are also consistent with our findings that sustained MPK3/6 activities concern chiefly MPK3, and are dependent in different extents on NDR1 and EDS1. Yet it must be reminded that the K3CA-2 and *mkk4mkk5* lines we used are not only affected in the pattern of sustained MPK3/6 activations but also in the pattern of transient activations. It is therefore not possible to rule out the possibility that the phenotypes we obtained for these lines are due to modifications not in sustained but transient MPK3/6 activations. As a matter of fact, the K3CA-2 and *mkk4mkk5* lines display similar resistance/susceptibility phenotypes in response to *Pst* AvrRps4 infiltration (Fig. S5), even if this strain does not provoke a strong sustained MPK3/6 activation (Fig. 1A, S1).

**NLR and NLR signaling contribute to the SA sector of defense downstream of MPK3 activation.**

The finding that MPK3 accumulates in the nucleus in response to *Pst* AvrRpt2 prompted us to look at the genes whose expressions are controlled by MPK3/6 activity. In previous works, we already established that expression of K3CA-2 leads to the upregulation of numerous *NLR* genes and assumed that these upregulations could be responsible for the SA-dependent auto-immune phenotype of K3CA-2 (Lang et al., 2017). This hypothesis was confirmed by the fact that mutation in the CNL SUMM2 partly reverts the K3CA-2 phenotype (Genot et al., 2017). To go further, we crossed K3CA-2 with the *ndr1-1* and *eds1-2* lines as well as with the *snc1-11* line which is impaired in the functions of SNC1, a TNL upregulated in the K3CA-2 transcriptome (Genot et al., 2017; Lang et al., 2017). As shown in Figure 4A, the developmental phenotype of K3CA-2 is partially reverted by the *snc1-11* and *ndr1-1* mutations, and totally by the *eds1-2* mutation. Then we analysed the expression levels of *PR1*, *SID2* and *PBS3* that are three different marker genes for the SA sector of defense. *PR1* is a characteristic SA-responsive gene (Tsuda et al., 2013) while *SID2* and *PBS3* code for enzymes involved in the synthesis of SA (Huang et al., 2020). In agreement with the developmental reversions, we found that the accumulations of these genes in K3CA-2 are

mildly reduced by the *snc1-11* and *ndr1-1* mutations, and drastically by the *eds1-2* mutation (Fig. 4B). Remarkably, when we analyzed the levels of MPK3 activity and quantity in the different lines, we observed that those remain globally the same in K3CA-2, K3CA-2/*snc1-11* and K3CA-2/*ndr1-1*, but considerably decrease in K3CA-2/*eds1-2* (Fig. 4C). Overall these findings confirm that NLRs like SNC1, and NLR signaling components like NDR1 can act downstream of MPK3 activity to promote the SA sector of defense. The K3CA-2 suppressor approach also highlights, in a more obvious fashion than in response to AvrRpt2 recognition (Fig. 2A, 2B, 2E), the original regulatory role of EDS1 which appears essential to achieve and maintain sufficiently high levels of active MPK3 to trigger the SA pathway of defense. Incidentally such a role which places EDS1 upstream of MPK3/6 is also compatible with the idea that EDS1 could drive a positive feedback loop downstream of MPK3/6 to ensure their sustainable activation.

**The NLRs *AT3G04220* and *AT4G11170* are upregulated both in ETI and PTI in a manner which is dependent on MPK3/6 activities, EDS1 and NDR1.**

To get a deeper understanding of the *NLR* upregulations mediated by MPK3/6 activities, we first compared our 20 candidate *NLR* genes from the K3CA-2 transcriptome (Genot et al., 2017; Lang et al., 2017) with genes upregulated by conditional expressions of constitutively active forms of *At*MKK4 (MKK4$^{DD}$) and its ortholog *Nt*MKK2 (MKK2$^{DD}$) (Su et al., 2018; Tsuda et al., 2013), and found 12 genes commonly upregulated in the three conditions. As the transcriptomic analyses were performed with plants of different ages, shortly after the expressions of MKK2$^{DD}$ and MKK4$^{DD}$ (6h and 24h respectively), the significant overlap we observed (12/20) tends to attest that *NLR* upregulation is not a pleitropic effect of K3CA-2 but rather a direct consequence of MPK3/6 activation. Then we compared the 12 *NLR* genes with a list of 55 *NLR* genes whose expressions were found to be induced in response to flg22 (Yu et al., 2013), as well as with a list of genes upregulated in the 24h post infiltration with the *Pst* AvrRpt2 and AvrRpm1 strains (Mine et al., 2018). Based on this, we ended up with seven *NLR* genes common to all conditions. These seven *NLRs* include five *TNLs* and two *CNLs* (Table 1), and represent *NLR* genes likely regulated by MPK3/6 during both PTI and ETI.

Next we compared, between Col-0 and *mkk4mkk5*, the expression levels of the seven *NLRs* in response to flg22 (1 hpi and 3 hpi) and *Pst* AvrRpt2 (5 hpi and 8 hpi). The results indicate that these genes are indeed specifically upregulated by the treatments although we can also notice some mild mock effect for some genes. In addition they globally confirm the positive effect of MKK4/5 on the *NLR* upregulation even if the differences between the two genotypes are not always statistically significant (Fig. 5). A reason for this could be that MPK3/6 activities are not totally abolished in *mkk4mkk5* or that other signaling pathways converge towards *NLR* upregulation and can compensate, in some extent, for MPK3/6 impairment.

To further study the roles of MPK3/6 activities on *NLR* upregulation, we performed an expression analysis for *AT3G04220* and *AT4G11170* (which are the two *NLRs* for which the contributions of MKK4/5 are the most obvious) in response to various treatments (infiltrations with *Pst* WT, AvrRpt2, AvrRpm1, AvrRps4, *hrcC-*, and mock) at 5 hpi and 8 hpi corresponding to timepoints where *Pst* AvrRpt2 and AvrRpm1, unlike other strains, induce high sustained MPK3/6 activations. In parallel we also measured the expression levels of the *PR1* gene as readout of the plant defense responses dependent on the SA pathway. Results revealed that globally the three genes are strongly upregulated by *Pst* AvrRpt2 and AvrRpm1, moderately by *Pst* AvrRps4 and weakly in response to *Pst* WT and *hrcC-,* at a level which is not distinguishable from the mock (Fig. 6A). From this, we inferred that the differences in the *AT3G04220*, *AT4G11170* and *PR1* inductions might be mostly due to the differences in MPK3/6 activations, and also that the sustained MPK3/6 activities observed in response to *Pst* AvrRpt2, AvrRpm1 and AvrRps4 reinforce the transcriptional effects of the sole transient activities caused by *Pst* WT and *hrcC-*.

To consolidate our interpretation, we investigated the expression levels of *AT3G04220*, *AT4G11170* and *PR1* in the XVE-AvrRpt2 lines. As shown in Figure 6B, the three genes are strongly upregulated upon estradiol treatment while the inductions are fully compromised in the *ndr1-1* background and partially in the *eds1-2* background. Given the contributions of NDR1 and EDS1 to the activations of MPK3/6 in response to AvrRpt2 (Fig. 2), these results are consistent with the notion that MPK3/6 activities, NDR1 and EDS1 act in the same signaling pathway to promote expression of *AT3G04220*, *AT4G11170* and *PR1* during AvrRpt2-triggered ETI.

Furthermore we measured the transcript levels of *AT3G04220*, *AT4G11170* and *PR1* in response to *Pst* AvrRpt2 in the Col-0, *mkk4mkk5*, *ndr1-1* and *eds1-2* backgrounds, and could show that proper induction of the three genes does require functional MKK4/5, NDR1 and EDS1 (Fig. 6C). We also noticed differences in the contributions of these components to the *NLR* and *PR1* inductions, that of MKK4/5 being weaker than that of EDS1 which in turn is weaker than that of NDR1. Considering that the impact of MKK4/5 on sustained MPK3/6 activities appears stronger than that of EDS1 (Fig. 2B, S4), such differences were not entirely anticipated. An explanation could be, as mentionned previously, that other factors downstream of EDS1 and NDR1, acting additionally to or buffering the MPK3/6 pathway are involved in the transcriptional regulation of the *NLR* and *PR1* genes in response to *Pst* AvrRpt2.

To confirm the role of sustained MPK3/6 activations, we also compared the inductions of *AT3G04220*, *AT4G11170* and *PR1* in response to *Pst* AvrRpm1 between Col-0 and *mkk4mkk5* and found that they are compromised in the latter background as they are in response to *Pst* AvrRpt2 (Fig. S6).

Finally we analyzed the expressions of *AT3G04220*, *AT4G11170* and *PR1* in the Col-0, *mkk4mkk5*, *ndr1-1* and *eds1-2* backgrounds in response to the PAMP flg22 at 2 hpi and 8 hpi. Surprisingly, in this condition, we established that loss of functions of not only MKK4/5, but also of NDR1 and EDS1 impair the upregulation of the *NLR* genes as well as that of *PR1* (Fig. 6D). Since EDS1 and NDR1 are not involved in the transient flg22-mediated MPK3/6 activation (Fig. 2F), these findings uncover an unexpected role for the two ETI regulators in some PTI responses independently or downstream of MPK3/6. Interestingly we also found that in response to flg22, expression levels of *EDS1* and *NDR1* are increased but that these increases are compromised in the *mkk4mkk5* background comparatively to Col-0 (Fig. 7). These data further argue in favor of a model in which, during PTI, MPK3/6 activities contribute to the *NLR* upregulation upstream of EDS1 and NDR1.

**Upregulation of *AT3G04220* is sufficient to activate the SA sector of defense**

In order to determine what the effects of *NLR* upregulation can be, we first performed some pathoassays in *at3g04220* and *at4g11170* lines comparatively to Col-0 in response to *Pst* WT. However we could not detect any significant differences in the load of pathogens between the different genotypes, although other studies succeeded in showing that *at4g11170* is more sensitive than WT (Halter et al., 2021).

As an alternative we created two independent transgenic *Arabidopsis* lines expressing the coding sequence of *AT3G04220* in the *at3g04220* background, under the control of a dexamethasone-inducible promoter (DEX-*AT3G04220*/*at3g04220* lines). RT-qPCR experiments revealed that the two lines display a leaky expression of the *NLR* but still specifically respond to dexamethasone treatment with an induction of more than ten folds (Fig. 8). Then we measured in these two lines and the *at3g04220* mutant, the expression levels of the SA markers *PR1* and *PBS3* in response to dexamethasone or mock. We could show that induction of *AT3G04220* is correlated with the high inductions of the two SA marker genes, in a manner which seems dose- and time-dependent (Fig. 8). As the inductions are not observed in the *at3g04220* background, these findings strongly indicate that control of *AT3G04220* expression levels is critical to modulate SA-related defense responses.

We then evaluated the SA sector of defense in Col-0, *at3g04220* and *at4g11170* lines upon infiltration with *Pst* AvrRpt2 and flg22, through the expression levels of *SID2*, *PBS3*, *PR1* and *CBP60g*. *CBP60g* is a transcription factor acting as a master regulator of SA synthesis and signaling (Huang et al., 2020). However we could not detect any significant differences between the three genotypes in these conditions (Fig. S7). This result is actually not totally surprising. Indeed as we showed in this study, several NLRs are upregulated during PTI and ETI, therefore, when one is missing, others might take over and secure an appropriate implementation of the SA sector of defense. Incidentally the absence of difference between Col-0, *at3g04220* and *at4g11170* is consistent with the fact that we could not observe a higher susceptibility to *Pst* WT in the single mutants comparatively to Col-0. At last a recent study revealed that ectopic expression of both *AT3G04220* and *AT4G11170* in tobacco leaves lead to important accumulation of SA and cell death, while simultaneous depletion of multiple NLR levels through overexpression of the E3 ligase SNIPER1

compromizes SA-dependent PTI responses (Tian et al., 2021). Overall these data further support our own results and conclusions.

## Discussion

### Regulation of sustained and transient MPK3/6 activations

One of the first results we obtained by comparing the effects of different *Pst* strains expressing different effectors is that sustained activations of MPK3/6 are characteristic of ETI mediated by the CNLs RPS2 and RPM1 (Fig. 1A, 1B). Indeed, although sustained activation could also be detected in response to *Pst* AvrRps4, this one was significantly weaker and could not be associated for the moment with clear NLR receptor (Fig. 1A, S1). These findings are actually consistent with previous reports (Cui et al., 2017; Ngou et al., 2020; Su et al., 2018; Tsuda et al., 2013). An explanation for this characteristic could be that sustained MPK3/6 activities are mostly mediated by CNLs. Another possibility could be that sustained MPK3/6 activities are consecutive to the recognition of effectors acting at the level of the cell membrane, as it is the case for AvrRpt2 and AvrRpm1 which both target RIN4. In this model the mechanisms of sustained MPK3/6 activations would be reminiscent of those allowing transient activations (Lang and Colcombet, 2020).

We also demonstrated in our study that sustained MPK3/6 activations depend on NDR1 and EDS1 (Fig. 2). Because NDR1 is an integrin-like protein involved in the association between the plasma membrane and the cell wall, as well as a master regulator of the AvrRpt2- and AvrRpm1-triggered ETI (Knepper et al., 2011), it is not really surprising to find it upstream of sustained MPK3/6 activations. In AvrRpt2-triggered ETI, EDS1 is known to buffer the SA sector of defense (Bhandari et al., 2019; Venugopal et al., 2009), yet the underpinning molecular mechanisms remain enigmatic. Here our results suggest that EDS1 might act upstream of sustained MPK3/6 to fulfill this function, which is actually in line with the fact that sustained MPK3/6 activities can also buffer the SA sector of defense (Tsuda et al., 2013).

Three additional points are worth mentioning in regard of the regulation of MPK3/6 activations. First, EDS1 and NDR1 are not required for transient MPK3/6 activations (Fig. 2F), indicating that if both transient and sustained MPK3/6 activations could originate at the cell

membrane, there are some decisive discrepancies in the molecular mechanisms of these two phenomena. Second, the *ndr1-1* mutation partially reverts the K3CA-2 phenotype (Fig. 4), strongly suggesting that the NLR signaling component NDR1 acts both upstream and downstream of sustained MPK3/6 activities. What could be the functions of NDR1 downstream of MPK3/6 is still to specify. Last, the *eds1-2* mutation compromizes the levels of K3CA-2 abundance and activity (Fig. 4C), hinting that EDS1 might be involved in a positive feedback regulation downstream of MPK3 activations allowing the high and sustainable accumulation of the active kinase. This could actually be in line with the model where sustained MPK3/6 activations are achieved through a regulatory loop dependent on Systemic-Acquired-Resistance (Wang et al., 2018).

**Functions of sustained and transient MPK3/6 activations**

The question whether sustained MPK3/6 activations can give way to new functions comparatively to transient activations is unclear (Lang and Colcombet, 2020). Here we provided evidence that *NLR* upregulation controlled by MPK3/6 is not imputable to a specific pattern of activation, but that both transient and sustained MPK3/6 activations are proficient in it (Fig. 5, 6). Moreover our results suggest that sustained activation caused by specific pathogen strains could reinforce the effects of transient activation on *NLRs* and *PR1* expressions (Fig. 6A). However a full understanding of how the transition between transient MPK3/6 activation, elicited by PAMP perception, and sustained activation, elicited by effector recognition, converges towards the *NL*R upregulations, and thereby impacts the strenght of the defense responses is still missing. This is notably a reason why we could not conclude about the resistance phenotypes of lines affected in the same time in the transient and sustained pattern of MPK3/6 activities (Fig.3, S4, S5).

If MPK3/6 activities positively control the upregulations of some *NLR* genes, the mechanisms underlying these processes are for the moment unknown. Interestingly the inductions of *AT3G04220* and *AT4G11170* in response to flg22 have been shown to be regulated by promoter DNA methylation and the actions of WRKY transcription factors (TFs) (Halter et al., 2021; Yu et al., 2013). Since the functions of WRKY TFs are known to be modulated by MPK3/6, either as direct substrates or through the actions of VQ-domain containing proteins (Weyhe et al., 2014), further investigations in the links between these different actors seem

promising. An alternative could be that MPK3/6 activities inhibit the nonsense-mediated mRNA decay pathway which plays an important role for the regulation of *NLR* expression levels (Jung et al., 2020).

Our results (Fig. 6C, 6D) also leave room for the notion that other factors than MPK3/6 are instrumental in the upregulation of the *NLRs*. For instance Tian et al. showed that *TNL* inductions in PTI are compromised by inhibitor of calcium signaling, suggesting that CDPKs might as well be involved in these processes (Tian et al., 2021). The specificities of this pathway compared to the MAPK pathway remain to be elucidated.

**_NLR_ upregulation: a crosstalk between PTI and ETI**

Upregulations of *NLR* genes in a PTI context have already been documented in the past (Yu et al., 2013). Nevertheless a comprehensive analysis of the regulation and consequences of this phenomenon is still lacking. Here we demonstrated that MPK3/6, as well as the NLR signaling components EDS1 and NDR1 contribute to the upregulations of two *NLR* genes, *AT3G04220* and *AT4G11170*, upon both PAMP and effector treatments (Fig. 6). We further showed that upregulation of *AT3G04220* is sufficient to activate the SA sector of defense (Fig. 8). Altogether these results support the model presented in Fig. 9. In this one we propose that the transcriptional upregulation of some *NLR* genes would result in higher protein levels which, once above a certain threshold, would be sufficient to trigger autoactivation, irrespectively of pathogen effectors. Thereby MPK3/6 activities would bridge PTI and ETI by regulating *NLR* expression levels, and allowing modulation or « priming » of NLR activation in response not only to effectors, but also to PAMPs. As a consequence these NLRs should play a critical role during PTI. Remarkably a concomitant and independent study obtained similar results and came to similar conclusions (Tian et al., 2021). By revealing that TNL accumulation as well as several TNL signaling components, including EDS1, are required to mount an efficient SA-dependent PTI response, the authors of this study pinpointed the same crosstalk between PTI and ETI as we did. However they interpreted the need of TNL signaling components as a downstream event of TNL activation whereas our own data indicate that the NLR signaling components NDR1 and EDS1 might contribute to NLR activation through *NLR* upregulation.

Overall our findings bring new perspectives to the emerging model of the plant immune system in which defense responses are extensively and dynamically modulated by diverse interactions between PTI and ETI (Lu and Tsuda, 2020; Yuan et al., 2021b). They also raise important questions that await answers. One that seems of the utmost interest is related to the way components of NLR signaling promote *NLR* upregulations during PTI. As elements of answers, our results indicate that EDS1 and NDR1 do not affect transient MPK3/6 activations during PTI but that their expression levels are increased in a MPK3/6-dependent manner (Fig. 2F, 7), suggesting that in this context, and contrary to ETI, MPK3/6 contributes to *NLR* upregulation upstream of EDS1 and NDR1 (Fig. 9). However, we cannot either totally exclude the possibility that EDS1 and NDR1 would act on *NLR* upregulation independently of MPK3/6 activities through a process which would be reinforced by the promotion of EDS1 and NDR1 expression. Interestingly a recent report demonstrated that EDS1 could interact with some LRR-RPs as well as some RLCKs, and contribute to the PAMP-triggered ethylene accumulation, offering thereby an explanatory framework, based on physical mechanisms, for the link between ETI components and PTI responses (Pruitt et al., 2021). In the same order of idea, it was shown that NDR1 can interact with RIN4 (Day et al., 2006) that can interact with RPS2 (Mackey et al., 2003) that can interact with FLS2, the LRR-RK responsible for perceiving flg22 (Qi et al., 2011). Taken together these data outline a complex membrane-associated signalosome machinery that entangles components of both PTI and ETI (Dongus and Parker, 2021; Lu and Tsuda, 2020). Unravelling the complexity of this machinery would constitute a great step forward for the understanding of plant immune responses.

**Supplementary Data**

*Table S1.* Sequences of primers used for qPCR experiments.

*Fig. S1.* Sustained MAPK activation is characteristic of RPS2/RPM1-mediated ETI responses.

*Fig. S2. AvrRpt2* induction in the XVE-AvrRpt2 lines.

*Fig. S3.* flg22-mediated vs mock-mediated MPK3/6 activation.

*Fig. S4.* Misregulation of MPK3/6 activities in K3CA-2, *mpk3-1*, *mpk6-4* and *mkk4mkk5* lines.

*Fig. S5.* Resistance phenotypes against the *Pst* AvrRps4 strain.

*Fig. S6.* Upregulation of *AT3G04220*, *AT4G11170* and *PR1* in response to *Pst* AvrRpm1 infiltration in Col-0 and *mkk4mkk5*.

*Fig. S7*: Expression analysis of the SA sector of defense in Col-0, *at3g04220* and *at4g11170*.

**Data Availability Statement**

Data supporting the findings of this study are available within the paper and within its supplementary materials published online. The data concerning the biological replicates are available from the corresponding author, (Julien Lang), upon request.

**Aknowledgements**

The authors would like to thank Drs. Kenishi Tsuda and Wei Zhang for sharing plant and bacterial materials. This study was supported by the French INRAE.

**Author Contributions**

JL, through insightful discussions with JC, designed the experimental setups and processed the data. JL, BG and JB performed the experiments. JL wrote the manuscript with contributions of JB and JC.

**References**


Aarts, N., Metz, M., Holub, E., Staskawicz, B. J., Daniels, M. J., and Parker, J. E. (1998). Different requirements for EDS1 and NDR1 by disease resistance genes define at least two R gene-mediated signaling pathways in Arabidopsis. *Proceedings of the National Academy of Sciences of the United States of America*, *95*(17), 10306–10311. https://doi.org/10.1073/pnas.95.17.10306

Asai, T., Tena, G., Plotnikova, J., Willmann, M. R., Chiu, W.-L., Gomez-Gomez, L., Boller, T., Ausubel, F. M., and Sheen, J. (2002). MAP kinase signalling cascade in Arabidopsis innate immunity. *Nature*, *415*(6875), 977–983. https://doi.org/10.1038/415977a

Bartsch, M., Gobbato, E., Bednarek, P., Debey, S., Schultze, J. L., Bautor, J., and Parker, J. E. (2006). Salicylic acid-independent ENHANCED DISEASE SUSCEPTIBILITY1 signaling in Arabidopsis immunity and cell death is regulated by the monooxygenase FMO1 and the Nudix hydrolase NUDT7. *Plant Cell*, *18*(4), 1038–1051. https://doi.org/10.1105/tpc.105.039982

Belkhadir, Y., Nimchuk, Z., Hubert, D. A., David Mackey, D., and Dangl, J. L. (2004). Arabidopsis RIN4 Negatively Regulates Disease Resistance Mediated by RPS2 and RPM1 Downstream or Independent of the NDR1 Signal Modulator and Is Not Required for the Virulence Functions of Bacterial Type III Effectors AvrRpt2 or AvrRpm1. *Plant Cell*, *16*(10), 2822-2835. https://10.1105/tpc.104.024117

Bhandari, D. D., Lapin, D., Kracher, B., von Born, P., Bautor, J., Niefind, K., and Parker, J. E. (2019). An EDS1 heterodimer signalling surface enforces timely reprogramming of immunity genes in Arabidopsis. *Nature Communications*, *10*(1). https://doi.org/10.1038/s41467-019-08783-0

Bigeard, J., Colcombet, J., and Hirt, H. (2015). Signaling Mechanisms in Pattern-Triggered Immunity (PTI). *Molecular Plant*, *8*(4), 521–539. https://doi.org/10.1016/j.molp.2014.12.022

Century, K. S., Holub, E. B., and Staskawicz, B. J. (1995). NDR1, a locus of Arabidopsis thaliana that is required for disease resistance to both a bacterial and a fungal pathogen. *Proceedings of the National Academy of Sciences*, *92*(14), 6597 LP – 6601. https://doi.org/10.1073/pnas.92.14.6597

Colcombet, J., and Hirt, H. (2008). Arabidopsis MAPKs: a complex signalling network involved in multiple biological processes. *Biochemical Journal*, *413*(2), 217–226. https://doi.org/10.1042/BJ20080625

Cui, H., Gobbato, E., Kracher, B., Qiu, J., Bautor, J., and Parker, J. E. (2017). A core function of EDS1 with PAD4 is to protect the salicylic acid defense sector in Arabidopsis immunity. *New Phytologist*, *213*(4), 1802–1817. https://doi.org/10.1111/nph.14302

Cui, H., Tsuda, K., and Parker, J. E. (2015). Effector-Triggered Immunity: From Pathogen Perception to Robust Defense. *Annual Review of Plant Biology*, *66*(1), 487–511. https://doi.org/10.1146/annurev-arplant-050213-040012

Day, B., Dahlbeck, D., and Staskawicz, B. J. (2006). NDR1 Interaction with RIN4 Mediates the Differential Activation of Multiple Disease Resistance Pathways in andlt;emandgt;Arabidopsisandlt;/emandgt; *The Plant Cell*, *18*(10), 2782 LP – 2791. https://doi.org/10.1105/tpc.106.044693

Dóczi, R., and Bögre, L. (2018). The Quest for MAP Kinase Substrates: Gaining Momentum. *Trends in Plant Science*, *23*(10), 918–932. https://doi.org/10.1016/j.tplants.2018.08.002

Dongus, J. A., and Parker, J. E. (2021). EDS1 signalling: At the nexus of intracellular and surface receptor immunity. *Current Opinion in Plant Biology*, *62*, 102039. https://doi.org/https://doi.org/10.1016/j.pbi.2021.102039

Frei dit Frey, N., Garcia, A. V., Bigeard, J., Zaag, R., Bueso, E., Garmier, M., Pateyron, S., de Tauzia-Moreau, M.-L., Brunaud, V., Balzergue, S., et al. (2014). Functional analysis of Arabidopsisimmune-related MAPKs uncovers a role for MPK3 as negative regulator of inducible defences. *Genome Biology*, *15*(6), R87. https://doi.org/10.1186/gb-2014-15-6-r87

Gao, M., Liu, J., Bi, D., Zhang, Z., Cheng, F., Chen, S., and Zhang, Y. (2008). MEKK1, MKK1/MKK2 and MPK4 function together in a mitogen-activated protein kinase cascade to regulate innate immunity in plants. *Cell Research*, *18*(12), 1190–1198. https://doi.org/10.1038/cr.2008.300

Gao, X., Chen, X., Lin, W., Chen, S., Lu, D., Niu, Y., Li, L., Cheng, C., McCormack, M., Sheen, J., et al.. (2013). Bifurcation of Arabidopsis NLR immune signaling via $Ca^{2+}$-dependent protein kinases. *PLoS Pathogens*, *9*(1), e1003127. https://doi.org/10.1371/journal.ppat.1003127

Genot, B., Lang, J., Berriri, S., Garmier, M., Gilard, F., Pateyron, S., Haustraete, K., Van Der Streaten, D., Hirt, H., and Colcombet, J. (2017). Constitutively active arabidopsis MAP kinase 3 triggers defense responses involving salicylic acid and SUMM2 resistance protein. *Plant Physiology*, *174*(2), 1238–1249. https://doi.org/10.1104/pp.17.00378

Halter, T., Wang, J., Amesefe, D., Lastrucci, E., Charvin, M., Singla Rastogi, M., and Navarro, L. (2021). The Arabidopsis active demethylase ROS1 cis-regulates defence genes by erasing DNA methylation at promoter-regulatory regions. *ELife*, *10*. https://doi.org/10.7554/eLife.62994

Harris, J. M., Balint-Kurti, P., Bede, J. C., Day, B., Gold, S., Goss, E. M., Grenville-Briggs, L. J., Jones, K. M., Wang, A., Wang, Y., et al. (2020). What are the Top 10 Unanswered Questions in Molecular Plant-Microbe Interactions? *Molecular Plant-Microbe Interactions®*, *33*(12), 1354–1365. https://doi.org/10.1094/MPMI-08-20-0229-CR

Huang, W., Wang, Y., Li, X., and Zhang, Y. (2020). Biosynthesis and Regulation of Salicylic Acid and N-Hydroxypipecolic Acid in Plant Immunity. *Molecular Plant*, *13*(1), 31–41. https://doi.org/10.1016/j.molp.2019.12.008

Ichimura, K., Shinozaki, K., Tena, G., Sheen, J., Henry, Y., Champion, A., Kreis, M., Zhang, S., Hirt, H., Wilson, C., et al. (2002). Mitogen-activated protein kinase cascades in plants: a new nomenclature. *Trends in Plant Science*, *7*(7), 301–308.

https://doi.org/10.1016/S1360-1385(02)02302-6

Jones, J.D.G., D. J. L. (2006). The Plant Immune System. *Nature*, *444*, 323–329.

Jung, H. W., Panigrahi, G. K., Jung, G. Y., Lee, Y. J., Shin, K. H., Sahoo, A., Choi, E. S., Lee, E., Kim, K. M., Yang, S. H., et al. (2020). Pathogen-Associated Molecular Pattern-Triggered Immunity Involves Proteolytic Degradation of Core Nonsense-Mediated mRNA Decay Factors During the Early Defense Response. *Plant Cell*, *32*(4), 1081–1101. https://doi.org/10.1105/tpc.19.00631

Kapos, P., Devendrakumar, K. T., and Li, X. (2019). Plant NLRs: From discovery to application. *Plant Science*, *279*(November 2017), 3–18. https://doi.org/10.1016/j.plantsci.2018.03.010

Knepper, C., Savory, E. A., and Day, B. (2011). Arabidopsis NDR1 Is an Integrin-Like Protein with a Role in Fluid Loss and Plasma Membrane-Cell Wall Adhesion. *Plant Physiology*, *156*(1), 286 LP – 300. https://doi.org/10.1104/pp.110.169656

Lang, J., and Colcombet, J. (2020). Sustained Incompatibility between MAPK Signaling and Pathogen Effectors. *International Journal of Molecular Sciences*, *21*(21). https://doi.org/10.3390/ijms21217954

Lang, J., Genot, B., Hirt, H., and Colcombet, J. (2017). Constitutive activity of the Arabidopsis MAP Kinase 3 confers resistance to Pseudomonas syringae and drives robust immune responses. *Plant Signaling and Behavior*, *12*(8). https://doi.org/10.1080/15592324.2017.1356533

Li, S., Han, X., Yang, L., Deng, X., Wu, H., Zhang, M., Liu, Y., Zhang, S., and Xu, J. (2018). Mitogen-activated protein kinases and calcium-dependent protein kinases are involved in wounding-induced ethylene biosynthesis in Arabidopsis thaliana. *Plant, Cell and Environment*, *41*(1), 134–147. https://doi.org/10.1111/pce.12984

Lu, Y., and Tsuda, K. (2020). Intimate Association of PRR- and NLR-Mediated Signaling in Plant Immunity. *Molecular Plant-Microbe Interactions®*, *34*(1), 3–14. https://doi.org/10.1094/MPMI-08-20-0239-IA

Mackey, D., Belkhadir, Y., Alonso, J. M., Ecker, J. R., and Dangl, J. L. (2003). Arabidopsis RIN4 Is a Target of the Type III Virulence Effector AvrRpt2 and Modulates RPS2-Mediated Resistance. *Cell*, *112*(3), 379–389. https://doi.org/10.1016/S0092-8674(03)00040-0

Mine, A., Seyfferth, C., Kracher, B., Berens, M. L., Becker, D., and Tsuda, K. (2018). The defense phytohormone signaling network enables rapid, high-amplitude transcriptional reprogramming during effector-triggered immunity[OPEN]. *Plant Cell*, *30*(6), 1199–1219. https://doi.org/10.1105/tpc.17.00970

Ngou, B. P. M., Ahn, H.-K., Ding, P., and Jones, J. D. G. (2021). Mutual potentiation of plant immunity by cell-surface and intracellular receptors. *Nature*. https://doi.org/10.1038/s41586-021-03315-7

Ngou, B. P. M., Ahn, H. K., Ding, P., Redkar, A., Brown, H., Ma, Y., Youles, M., Tomlinson, L.,

and Jones, J. D. G. (2020). Estradiol-inducible AvrRps4 expression reveals distinct properties of TIR-NLR-mediated effector-triggered immunity. *Journal of Experimental Botany*, *71*(6), 2186–2197. https://doi.org/10.1093/jxb/erz571

Nobori, T., Velásquez, A. C., Wu, J., Kvitko, B. H., Kremer, J. M., Wang, Y., He, S. Y., and Tsuda, K. (2018). Transcriptome landscape of a bacterial pathogen under plant immunity. *Proceedings of the National Academy of Sciences of the United States of America*, *115*(13), E3055–E3064. https://doi.org/10.1073/pnas.1800529115

Peñaloza-Vázquez, A., Preston, G. M., Collmer, A., and Bender, C. L. (2000). Regulatory interactions between the Hrp type III protein secretion system and coronatine biosynthesis in Pseudomonas syringae pv. tomato DC3000. *Microbiology*, *146*(10), 2447–2456. https://doi.org/https://doi.org/10.1099/00221287-146-10-2447

Peng, Y., Van Wersch, R., and Zhang, Y. (2018). Convergent and divergent signaling in PAMP-triggered immunity and effector-triggered immunity. *Molecular Plant-Microbe Interactions*, *31*(4), 403–409. https://doi.org/10.1094/MPMI-06-17-0145-CR

Pruitt, R. N., Locci, F., Wanke, F., Zhang, L., Saile, S. C., Joe, A., Karelina, D., Hua, C., Fröhlich, K., Wan, W.-L., et al. (2021). The EDS1-PAD4-ADR1 node mediates Arabidopsis pattern-triggered immunity. *Nature*, 598(7881):495-499. https://doi.org/10.1038/s41586-021-03829-0

Qi, Y., Tsuda, K., Glazebrook, J., and Katagiri, F. (2011). Physical association of pattern-triggered immunity (PTI) and effector-triggered immunity (ETI) immune receptors in Arabidopsis. *Molecular Plant Pathology*, *12*(7), 702–708. https://doi.org/10.1111/j.1364-3703.2010.00704.x

Saucet, S. B., Ma, Y., Sarris, P. F., Furzer, O. J., Sohn, K. H., and Jones, J. D. G. (2015). Two linked pairs of Arabidopsis TNL resistance genes independently confer recognition of bacterial effector AvrRps4. *Nature Communications*, *6*(1), 6338. https://doi.org/10.1038/ncomms7338

Su, J., Yang, L., Zhu, Q., Wu, H., He, Y., Liu, Y., Xu, J., Jiang, D., and Zhang, S. (2018). Active photosynthetic inhibition mediated by MPK3/MPK6 is critical to effector-triggered immunity. *PLoS Biology*, *16*(5), 1–29. https://doi.org/10.1371/journal.pbio.2004122

Sun, T., Nitta, Y., Zhang, Q., Wu, D., Tian, H., Lee, J. S., and Zhang, Y. (2018). Antagonistic interactions between two MAP kinase cascades in plant development and immune signaling. *EMBO Reports*, *19*(7), e45324. https://doi.org/10.15252/embr.201745324

Tian, H., Wu, Z., Chen, S., Ao, K., Huang, W., Yaghmaiean, H., Sun, T., Xu, F., Zhang, Y., Wang, S., et al. (2021). Activation of TIR signaling boosts pattern-triggered immunity. *Nature*, 598(7881):500-503. https://doi.org/ 10.1038/s41586-021-03987-1

Tsuda, K., Sato, M., Stoddard, T., Glazebrook, J., and Katagiri, F. (2009). Network properties of robust immunity in plants. *PLoS Genetics*, *5(12)*. https://doi: 10.1371/journal.pgen.1000772

Tsuda, K., and Katagiri, F. (2010). Comparing signaling mechanisms engaged in pattern-triggered and effector-triggered immunity. In *Current Opinion in Plant Biology* (Vol. 13,

Issue 4, pp. 459–465). https://doi.org/10.1016/j.pbi.2010.04.006

Tsuda, K., Mine, A., Bethke, G., Igarashi, D., Botanga, C. J., Tsuda, Y., Glazebrook, J., Sato, M., and Katagiri, F. (2013). Dual Regulation of Gene Expression Mediated by Extended MAPK Activation and Salicylic Acid Contributes to Robust Innate Immunity in Arabidopsis thaliana. *PLoS Genetics*, *9*(12). https://doi.org/10.1371/journal.pgen.1004015

Venugopal, S. C., Jeong, R. D., Mandal, M. K., Zhu, S., Chandra-Shekara, A. C., Xia, Y., Hersh, M., Stromberg, A. J., Navarre, D. R., Kachroo, A., and Kachroo, P. (2009). Enhanced disease susceptibility 1 and salicylic acid act redundantly to regulate resistance gene-mediated signaling. *PLoS Genetics*, *5*(7), 22–24. https://doi.org/10.1371/journal.pgen.1000545

Wang, Y., Schuck, S., Wu, J., Yang, P., Döring, A. C., Zeier, J., and Tsuda, K. (2018). A mpk3/6-wrky33-ald1-pipecolic acid regulatory loop contributes to systemic acquired resistance[open]. *Plant Cell*, *30*(10), 2480–2494. https://doi.org/10.1105/tpc.18.00547

Weyhe, M., Eschen-Lippold, L., Pecher, P., Scheel, D., and Lee, J. (2014). Ménage à trois: The complex relationships between mitogen-activated protein kinases, WRKY transcription factors, and VQ-motif-containing proteins. *Plant Signaling and Behavior*, *9*(JUN), 20–24. https://doi.org/10.4161/psb.29519

Wu, Z., Li, M., Dong, O. X., Xia, S., Liang, W., Bao, Y., Wasteneys, G., and Li, X. (2019). Differential regulation of TNL-mediated immune signaling by redundant helper CNLs. *The New Phytologist*, *222*(2), 938–953. https://doi.org/10.1111/nph.15665

Xu, J., Li, Y., Wang, Y., Liu, H., Lei, L., Yang, H., Liu, G., and Ren, D. (2008). Activation of MAPK Kinase 9 Induces Ethylene and Camalexin Biosynthesis and Enhances Sensitivity to Salt Stress in Arabidopsis*. *Journal of Biological Chemistry*, *283*(40), 26996–27006. https://doi.org/https://doi.org/10.1074/jbc.M801392200

Xu, J., Meng, J., Meng, X., Zhao, Y., Liu, J., Sun, T., Liu, Y., Wang, Q., and Zhang, S. (2016). Pathogen-Responsive MPK3 and MPK6 Reprogram the Biosynthesis of Indole Glucosinolates and Their Derivatives in Arabidopsis Immunity. *The Plant Cell*, *28*(5), 1144 LP – 1162. https://doi.org/10.1105/tpc.15.00871

Yu, A., Lepère, G., Jay, F., Wang, J., Bapaume, L., Wang, Y., Abraham, A.-L., Penterman, J., Fischer, R. L., Voinnet, O., and Navarro, L. (2013). Dynamics and biological relevance of DNA demethylation in Arabidopsis antibacterial defense. *Proceedings of the National Academy of Sciences of the United States of America*, *110*(6), 2389–2394. https://doi.org/10.1073/pnas.1211757110

Yuan[a], M., Jiang, Z., Bi, G., Nomura, K., Liu, M., Wang, Y., Cai, B., Zhou, J.-M., He, S. Y., and Xin, X.-F. (2021). Pattern-recognition receptors are required for NLR-mediated plant immunity. *Nature*. https://doi.org/10.1038/s41586-021-03316-6

Yuan[b], M., Ngou, B. P. M., Ding, P., and Xin, X.-F. (2021). PTI-ETI crosstalk: an integrative view of plant immunity. *Current Opinion in Plant Biology*, *62*, 102030. https://doi.org/10.1016/j.pbi.2021.102030

Zhao, C., Nie, H., Shen, Q., Zhang, S., Lukowitz, W., and Tang, D. (2014). EDR1 Physically Interacts with MKK4/MKK5 and Negatively Regulates a MAP Kinase Cascade to Modulate Plant Innate Immunity. *PLOS Genetics*, *10*(5), 1–11. https://doi.org/10.1371/journal.pgen.1004389

Zipfel, C. (2014). Plant pattern-recognition receptors. *Trends in Immunology*, *35*(7), 345–351. https://doi.org/10.1016/j.it.2014.05.004

## Tables

| Gene | Protein description |
|---|---|
| *AT1G12290* | CC-NBS-LRR class, localized at the plasma membrane |
| *AT4G11170* | TIR-NBS-LRR class (Resistance Methylated Gene 1, RMG1) |
| *AT3G04220* | TIR-NBS-LRR class |
| *AT5G41750* | TIR-NBS-LRR class |
| *AT1G66090* | TIR-NBS-LRR class |
| *AT1G15890* | CC-NBS-LRR class |
| *AT1G57630* | TIR-domain containing protein |

**Table 1: List of *NLR* genes upregulated by K3CA-2, MKK4/5, flg22, AvrRpt2 and AvrRpm1.** *NLR* genes commonly upregulated by K3CA-2 (Genot et al., 2017; Lang et al., 2017), *Nt*MKK2$^{DD}$ (Su, et al., 2018), *At*MKK4$^{DD}$ (Tsuda et al., 2013), flg22 treatment (Yu et al., 2013), and *Pst* AvrRpt2 and AvrRpm1 infiltrations (Mine et al., 2018). Descriptions were retrieved from TAIR (https://www.arabidopsis.org/index.jsp).

## Figure Legends

**Figure 1: Sustained MAPK activation is characteristic of RPS2/RPM1-mediated ETI responses, concerns mostly MPK3 and leads to a nuclear accumulation of MPK3.** MPK3/6 activities and quantities were analyzed through immunoblotting with anti-pTpY, anti-MPK3 and anti-MPK6 antibodies in Col-0 in response to various *Pst* strains **(A)**, in Col-0 and *rps2rpm1* backgrounds in response to *Pst* AvrRpt2 and AvrRpm1 **(B)**, and in total fraction (TF), nuclei-depleted fraction (ND) and nuclei-enriched fraction (NE) from Col-0 plants in response to mock or *Pst* AvrRpt2 (8 hpi) **(C)**. Coomassie stainings of blots serve as loading controls (LC). pMPK3 and pMPK6 stand for the phosphorylated active forms of MPK3 and MPK6. Immunoblottings with anti-H3 and anti-PEPC antibodies serve as markers for the nuclear and cytoplasmic fractions respectively. Values (Means ± SDs) indicate MPK3 fold change between mock and AvrRpt2 samples, and were calculated from 3 independent experiments using ImageJ software from non-saturated immunoblot pictures. All experiments were repeated at least 3 independent times with similar results.

**Figure 2: NDR1 and EDS1 contribute to sustained but not transient MAPK activation. (A)** MPK3/6 activities and quantities were analyzed through immunoblottings with anti-pTpY, anti-MPK3 and anti-MPK6 antibodies in different genetic backgrounds in response to *Pst* AvrRpt2. **(B)** Ratio of MPK3 activity in *ndr1-1* and *eds1-2* backgrounds comparatively to Col-0 in response to *Pst* AvrRpt2. Quantification was performed using ImageJ software from non-saturated immunoblot pictures of 3 independent replicates. Values of MPK3 activity were normalized by values of MPK3 abundance. The graph was drawn with the boxplot function from R. The box represents the 50% of the central data, with the line representing the median. The error bars represent the range of the data. **(C)**, **(D), (E), (F)** MPK3/6 activities and quantities were analyzed through immunoblotting with anti-pTpY, anti-MPK3 and anti-MPK6 antibodies in response to mock or *Pst* AvrRpt2 (8 hpi) in total fraction (TF), nuclei-depleted fraction (ND) and nuclei-enriched fraction (NE) from *ndr1-1* **(C)** and *eds1-2* **(D)**, or in response to estradiol in the XVE-AvrRpt2 backgrounds **(E)**, and in response to flg22 in Col-0, *ndr1-1* and *eds1-2* **(F)**. Coomassie stainings of blots serve as loading controls (LC). pMPK3 and pMPK6 stand for the phosphorylated active forms of MPK3 and MPK6. For **(C)** and **(D)**,

values (means ± half of the data range) indicate MPK3 fold change between mock and AvrRpt2 samples, and were calculated from 2 independent experiments using ImageJ software from non-saturated immunoblot pictures. Immunoblottings with anti-H3 and anti-PEPC antibodies serve as markers for the nuclear and cytoplasmic fractions respectively. All other experiments were repeated at least 3 independent times with similar results.

**Figure 3: Disturbed MAPK activities result in resistance/susceptibility phenotypes.** Plants were infiltrated with same amount of *Pst* AvrRpt2 and bacterial load was measured 3 days later. CFU means colony forming unit. Dotplot and histogram showing mean values and SDs for different genotypes were generated from data of at least 3 independent replicates. Letters indicate statistical significance (Kruskall-Wallis test followed by a nonparametric Tukey post-hoc test, $p<0.05$, $22<n<25$).

**Figure 4: NLR and NLR signaling contribute to the SA sector of defense downstream of MPK3 activation. (A)** Developmental reversion of the K3CA-2 phenotype by *ndr1-1*, *snc1-11* and *eds1-2*. Representative picture of 1.5 month old plants (left), and fresh weight (FW) mass of 1.5 month-old plants (right) are presented. The graph was drawn with the boxplot function from R. The box represents the 50% of the central data, with the line representing the median. The error bars represent the range of the data. Circles represent outlier data. Letters indicate statistical significance (Kruskall-Wallis test, followed by a nonparametric post-hoc Tukey test, $p<0.05$, $n=19$). **(B)** RT-qPCR experiments showing the relative expression levels of SA-related *PR1*, *PBS3* and *SID2* genes in different genetic backgrounds in 1.5 month-old plants. Mean values and SDs were calculated from 3 technical repeats. Letters indicate statistical differences (Kruskal-Wallis test followed by nonparametric post-hoc Tukey test, $p<0.05$, $n=3$). Experiments were repeated two independent times with similar results. **(C)** K3CA activity and quantity in different genetic backgrounds in 1.5 month-old plants were measured through an anti-myc immunoprecipitation followed by a kinase assay, and an immunoblotting with anti-myc antibodies. Coomassie staining of blot serves as a loading control (LC). Experiments were repeated at least 2 independent times with similar results.

**Figure 5: Expression of *NLR* genes is dependent on MPK3/6 activities in response to flg22 and *Pst* AvrRpt2.** Relative expression levels were measured through RT-qPCR experiments in response to flg22, *Pst* AvrRpt2 and mock at different timepoints. Mean values and SDs were calculated from 4 technical repeats. Letters indicate statistical differences (Wilcoxon-Mann-Whitney test, $p<0.05$, $n=4$), n.s. stands for not significative. Experiment was repeated two independent times with similar results.

**Figure 6: Upregulations of *AT3G04220*, *AT4G11170* and *PR1* are dependent on MPK3/6, NDR1 and EDS1.** Relative expression levels were measured at different timepoints through RT-qPCR experiments in Col-0 in response to various *Pst* strains **(A)**, in different XVE-AvrRpt2 lines in response to estradiol **(B)**, in Col-0 and different loss-of-function backgrounds in response to *Pst* AvrRpt2 infiltration **(C)**, and in response to flg22 **(D)**. Mean values and SDs were calculated from 3 technical repeats. Letters indicate statistical differences (Kruskal-Wallis test followed by nonparametric post-hoc Tukey test, $p<0.05$, $n=3$), n.s. stands for not significative. Experiments were repeated 2 independent times for **(A)** and at least 3 independent times for **(B)**, **(C)** and **(D)** with similar results.

**Figure 7: *EDS1* and *NDR1* are upregulated in response to flg22 in a *MKK4/5*-dependent manner.** Relative expression levels were measured through RT-qPCR experiments at different timepoints in Col-0 and *mkk4mkk5*. Mean values and SDs were calculated from 4 technical repeats. Letters indicate statistical differences (Wilcoxon-Mann-Whitney test, $p<0.05$, $n=4$), n.s. stands for not significative. Experiments were repeated 2 independent times with similar results.

**Figure 8: Upregulation of *AT3G04220* is sufficient to activate the SA sector of defense.** Relative expression levels were measured through RT-qPCR experiments in 2 independent DEX-AT3G04220/*at3g04220* lines and the *at3g04220* line at different timepoints and in

response to dexamethasone (+DEX) or mock. Mean values and SDs were calculated from 3 technical repeats. The experiment was repeated 3 independent times with similar results.

**Figure 9: PTI and ETI responses are intricated around the induction of *NLR* expression in a process involving MPK3/6 activation, and ETI signaling components EDS1 and NDR1.** In PTI context, upon PAMP perception by Pattern-Recognition Receptor (PRR), and signal transduction by Receptor-Like Cytoplasmic Kinases (RLCK), *NLR* upregulation is modulated by transient MPK3/6 activities, NDR1 and EDS1, with the two latters acting downstream or independently of the formers. In ETI context, the effectors AvrRpt2 and AvrRpm1, injected by the bacteria through a Type III Secretory System (T3SS) and targeting RIN4, are recognized by the CNLs RPS2 and RPM1, thereby triggering convergent signaling pathways involving NDR1, EDS1 as well as nuclei-accumulating and sustainably active MPK3/6, to further promote *NLR* expressions. Contrary to what happens in PTI, in ETI, NDR1 and EDS1 act upstream of sustained MPK3/6 activities. The recognition of other effectors, like AvrRps4, can also induce *NLR* expression but to a lesser extent, through the activation of the only EDS1 signaling branch. A positive feedback loop downstream of MPK3/6 and requiring EDS1 contributes to their sustained activation. Finally *NLR* transcriptional upregulation leads to the implementation of the SA sector of defense, through a NLR activation process which remains to be determined.

684

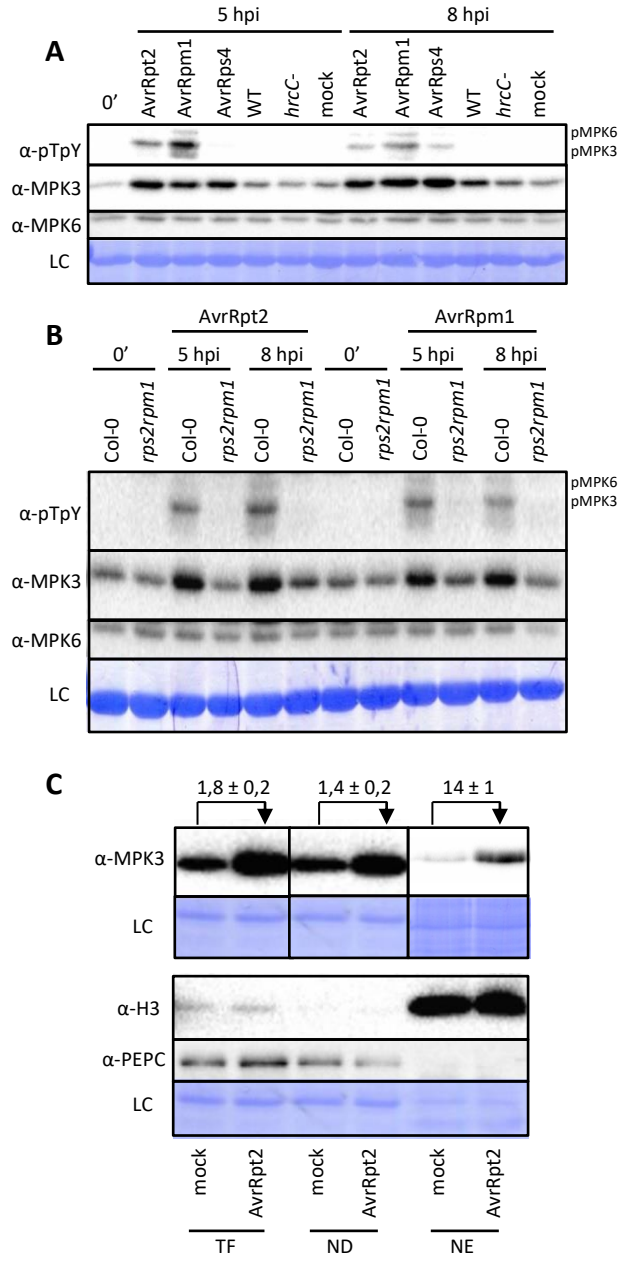


**Figure 1: Sustained MAPK activation is characteristic of RPS2/RPM1-mediated ETI responses, concerns mostly MPK3 and leads to a nuclear accumulation of MPK3.** MPK3/6 activities and quantities were analyzed through immunoblotting with anti-pTpY, anti-MPK3 and anti-MPK6 antibodies in Col-0 in response to various *Pst* strains **(A)**, in Col-0 and *rps2rpm1* backgrounds in response to *Pst* AvrRpt2 and AvrRpm1 **(B)**, and in total fraction (TF), nuclei-depleted fraction (ND) and nuclei-enriched fraction (NE) from Col-0 plants in response to mock or *Pst* AvrRpt2 (8 hpi) **(C)**. Coomassie stainings of blots serve as loading controls (LC). pMPK3 and pMPK6 stand for the phosphorylated active forms of MPK3 and MPK6. Immunoblottings with anti-H3 and anti-PEPC antibodies serve as markers for the nuclear and cytoplasmic fractions respectively. Values (Means ± SDs) indicate MPK3 fold change between mock and AvrRpt2 samples, and were calculated from 3 independent experiments using ImageJ software from non-saturated immunoblot pictures. All experiments were repeated at least 3 independent times with similar results.

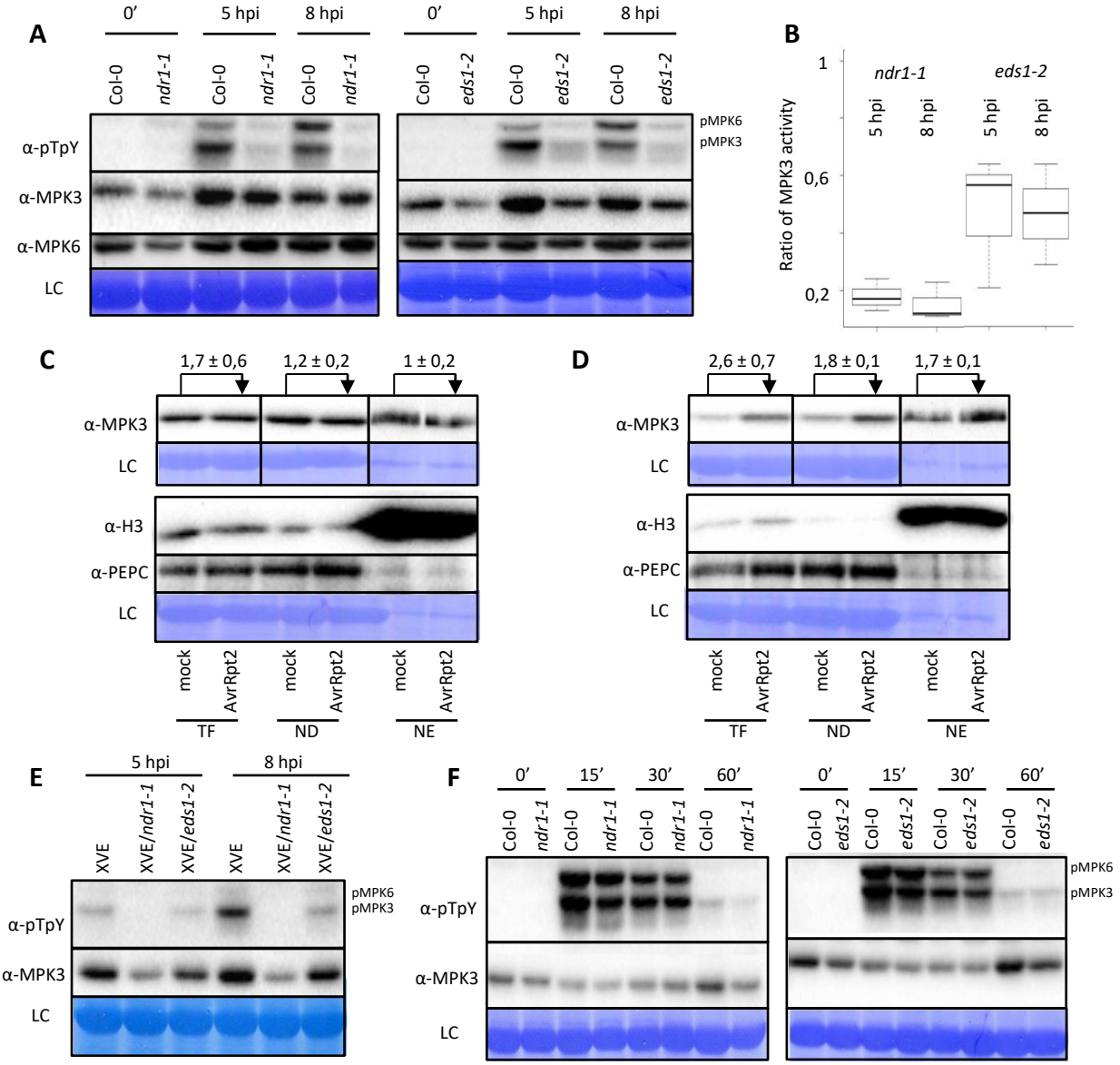


**Figure 2: NDR1 and EDS1 contribute to sustained but not transient MAPK activation. (A)** MPK3/6 activities and quantities were analyzed through immunoblottings with anti-pTpY, anti-MPK3 and anti-MPK6 antibodies in *ndr1-1* and *eds1-2* genetic backgrounds in response to *Pst* AvrRpt2. **(B)** Ratio of MPK3 activity in *ndr1-1* and *eds1-2* backgrounds comparatively to Col-0 in response to *Pst* AvrRpt2. Quantification was performed using ImageJ software from non-saturated immunoblot pictures of 3 independent replicates. Values of MPK3 activity were normalized by values of MPK3 abundance. The graph was drawn with the boxplot function from R. The box represents the 50% of the central data, with the line representing the median. The error bars represent the range of the data. **(C), (D), (E), (F)** MPK3/6 activities and quantities were analyzed through immunoblotting with anti-pTpY and anti-MPK3 antibodies in response to mock or *Pst* AvrRpt2 (8 hpi) in total fraction (TF), nuclei-depleted fraction (ND) and nuclei-enriched fraction (NE) from *ndr1-1* **(C)** and *eds1-2* **(D)**, or in response to estradiol in the XVE-AvrRpt2 backgrounds **(E)**, and in response to flg22 in Col-0, *ndr1-1* and *eds1-2* **(F)**. Coomassie stainings of blots serve as loading controls (LC). pMPK3 and pMPK6 stand for the phosphorylated active forms of MPK3 and MPK6. For **(C)** and **(D)**, values (means ± half of the data range) indicate MPK3 fold change between mock and AvrRpt2 samples, and were calculated from 2 independent experiments using ImageJ software from non-saturated immunoblot pictures. Immunoblottings with anti-H3 and anti-PEPC antibodies serve as markers for the nuclear and cytoplasmic fractions respectively. All other experiments were repeated at least 3 independent times with similar results.

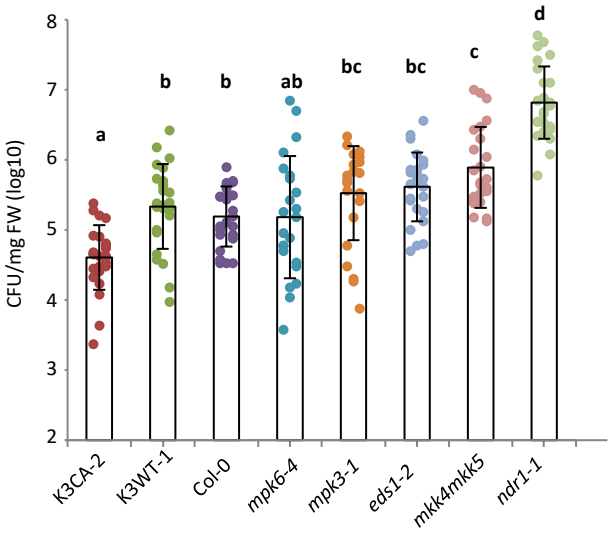


**Figure 3: Disturbed MAPK activities result in resistance/susceptibility phenotypes.** Plants were infiltrated with same amount of *Pst* AvrRpt2 and bacterial load was measured 3 days later. CFU means colony forming unit. Dotplot and histogram showing mean values and SDs for different genotypes were generated from data of at least 3 independent replicates. Letters indicate statistical significance (Kruskall-Wallis test followed by a nonparametric Tukey post-hoc test, $p<0.05$, $22<n<25$).

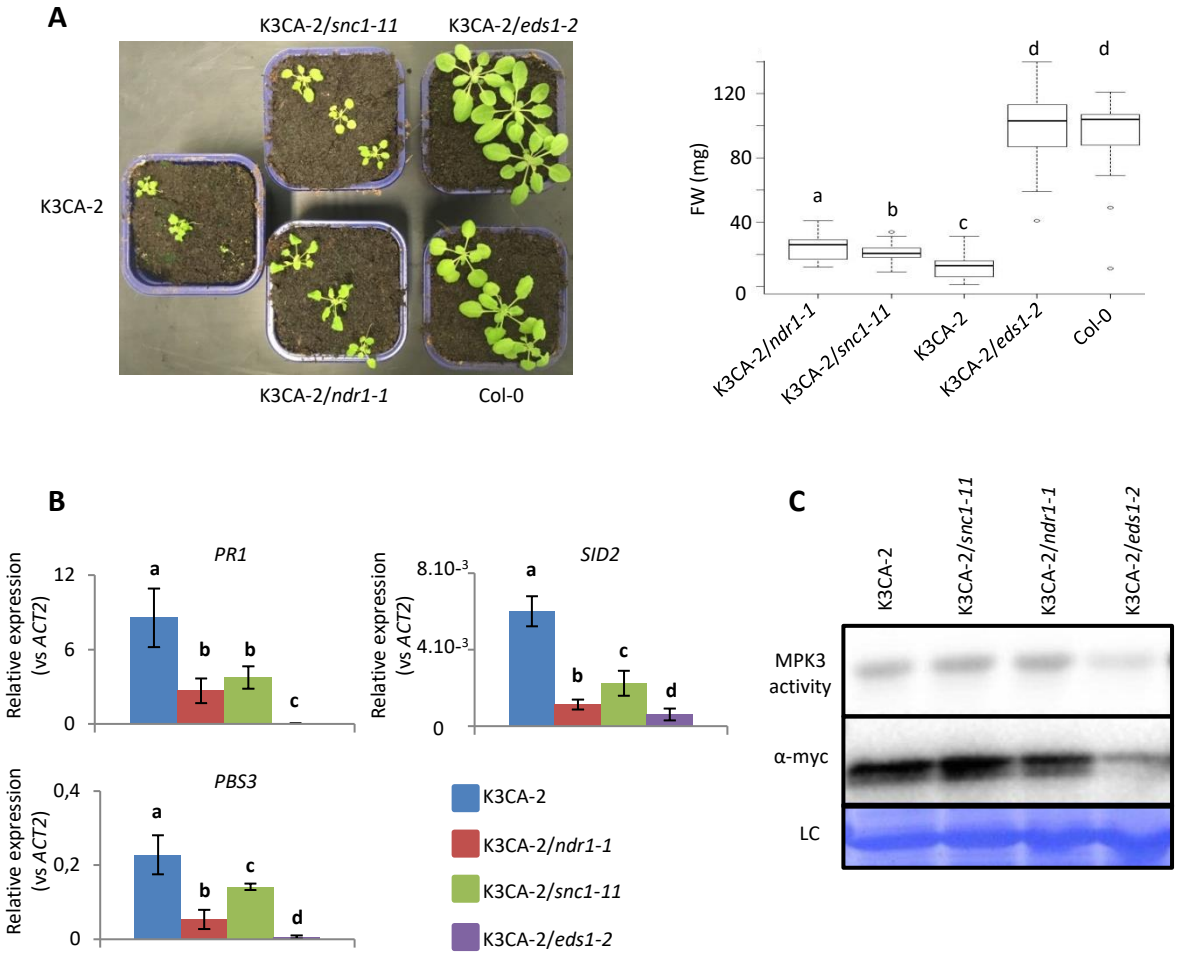


**Figure 4: NLR and NLR signaling contribute to the SA sector of defense downstream of MPK3 activation. (A)** Developmental reversion of the K3CA-2 phenotype by *ndr1-1*, *snc1-11* and *eds1-2*. Representative picture of 1.5 month old plants (left), and fresh weight (FW) mass of 1.5 month-old plants (right) are presented. The graph was drawn with the boxplot function from R. The box represents the 50% of the central data, with the line representing the median. The error bars represent the range of the data. Circles represent outlier data. Letters indicate statistical significance (Kruskall-Wallis test, followed by a nonparametric post-hoc Tukey test, $p<0.05$, $n=19$). **(B)** RT-qPCR experiments showing the relative expression levels of SA-related *PR1*, *PBS3* and *SID2* genes in different genetic backgrounds in 1.5 month-old plants. Mean values and SDs were calculated from 3 technical repeats. Letters indicate statistical differences (Kruskal-Wallis test followed by nonparametric post-hoc Tukey test, $p<0.05$, $n=3$). Experiments were repeated two independent times with similar results. **(C)** K3CA activity and quantity in different genetic backgrounds in 1.5 month-old plants were measured through an anti-myc immunoprecipitation followed by a kinase assay, and an immunoblotting with anti-myc antibodies. Coomassie staining of blot serves as a loading control (LC). Experiments were repeated at least 2 independent times with similar results.

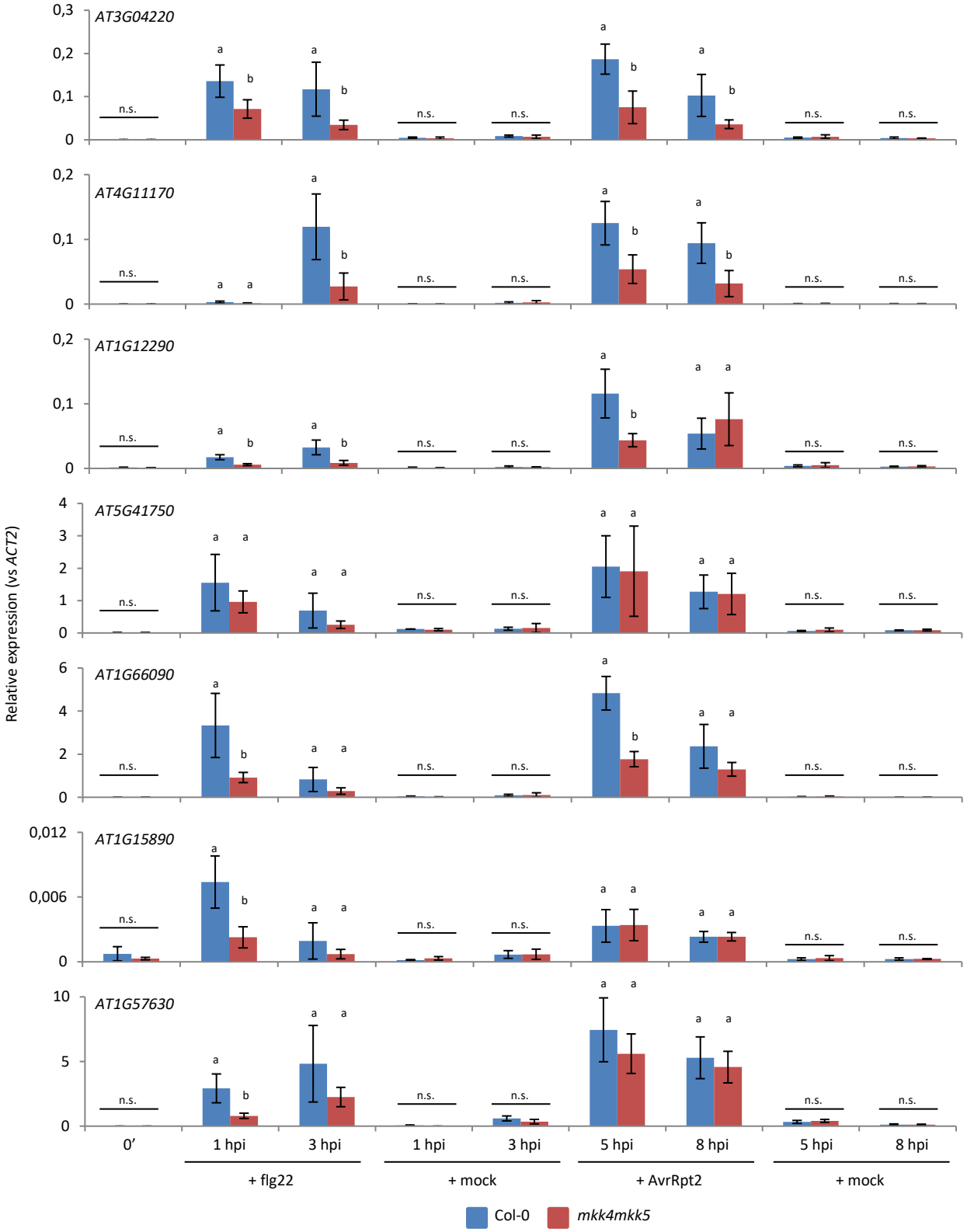


**Figure 5: Expression of *NLR* genes is dependent on MPK3/6 activities in response to flg22 and *Pst* AvrRpt2. .** Relative expression levels were measured through RT-qPCR experiments in response to flg22, *Pst* AvrRpt2 and mock at different timepoints. Mean values and SDs were calculated from 4 technical repeats. Letters indicate statistical differences (Wilcoxon-Mann-Whitney test, $p<0,05$, $n=4$), n.s. stands for not significative. Experiment was repeated two independent times with similar results.

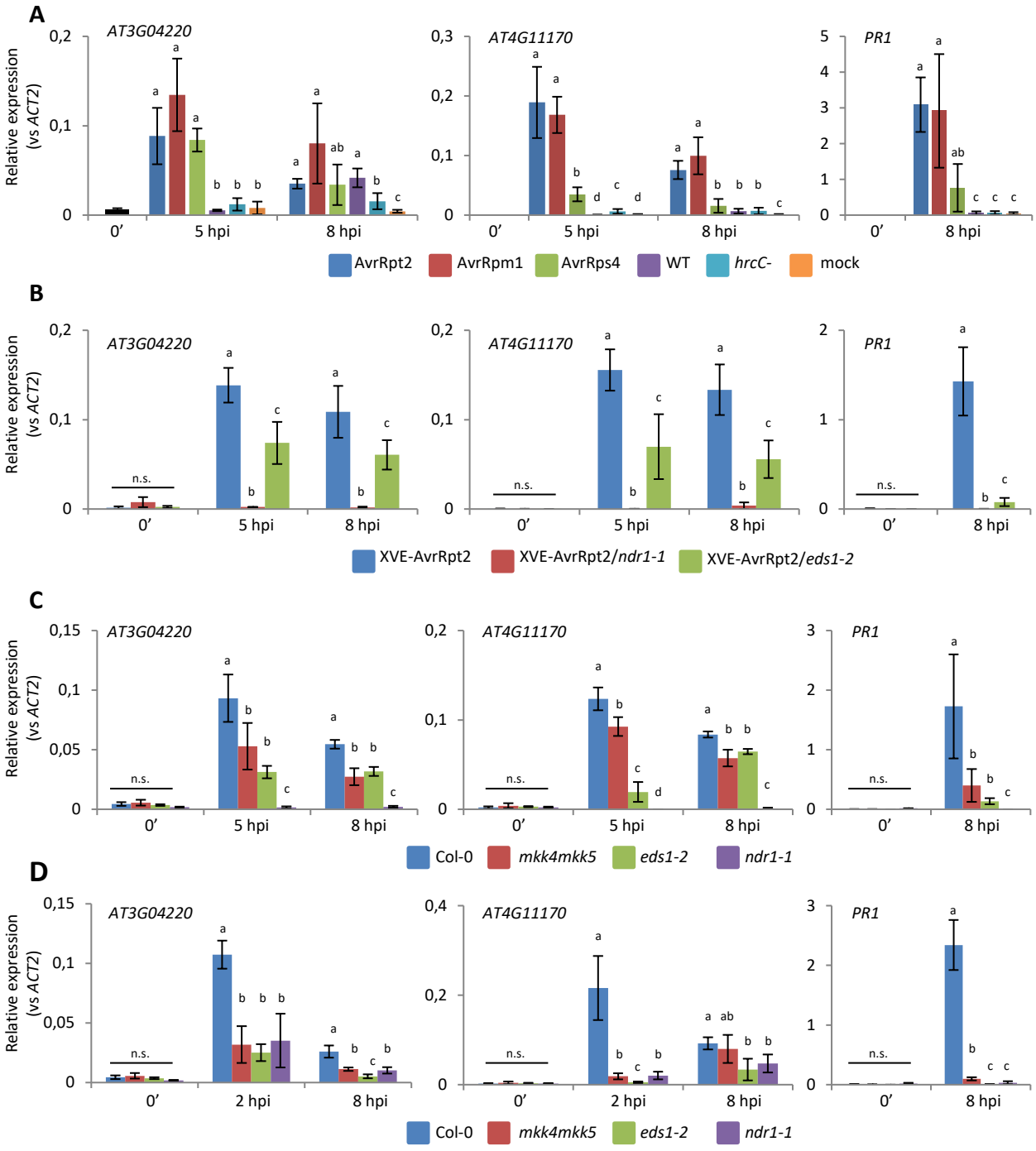


**Figure 6: Upregulations of *AT3G04220*, *AT4G11170* and *PR1* are dependent on MPK3/6, NDR1 and EDS1.** Relative expression levels were measured at different timepoints through RT-qPCR experiments in Col-0 in response to various *Pst* strains **(A)**, in different XVE-AvrRpt2 lines in response to estradiol **(B)**, in Col-0 and different loss-of-function backgrounds in response to *Pst* AvrRpt2 infiltration **(C)**, and in response to flg22 **(D)**. Mean values and SDs were calculated from 3 technical repeats. Letters indicate statistical differences (Kruskal-Wallis test followed by nonparametric post-hoc Tukey test, $p<0.05$, n=3), n.s. stands for not significative. Experiments were repeated 2 independent times for **(A)** and at least 3 independent times for **(B)**, **(C)** and **(D)** with similar results.

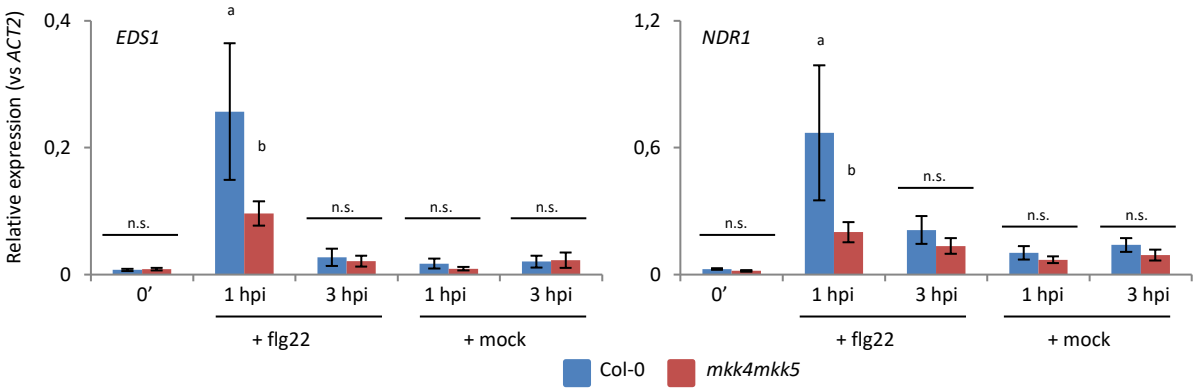


**Figure 7: *EDS1* and *NDR1* are upregulated in response to flg22 in a *MKK4/5*-dependent manner.** Relative expression levels were measured through RT-qPCR experiments at different timepoints in Col-0 and *mkk4mkk5*. Mean values and SDs were calculated from 4 technical repeats. Letters indicate statistical differences (Wilcoxon-Mann-Whitney test, $p<0,05$, $n=4$), n.s. stands for not significative. Experiments were repeated 2 independent times with similar results.

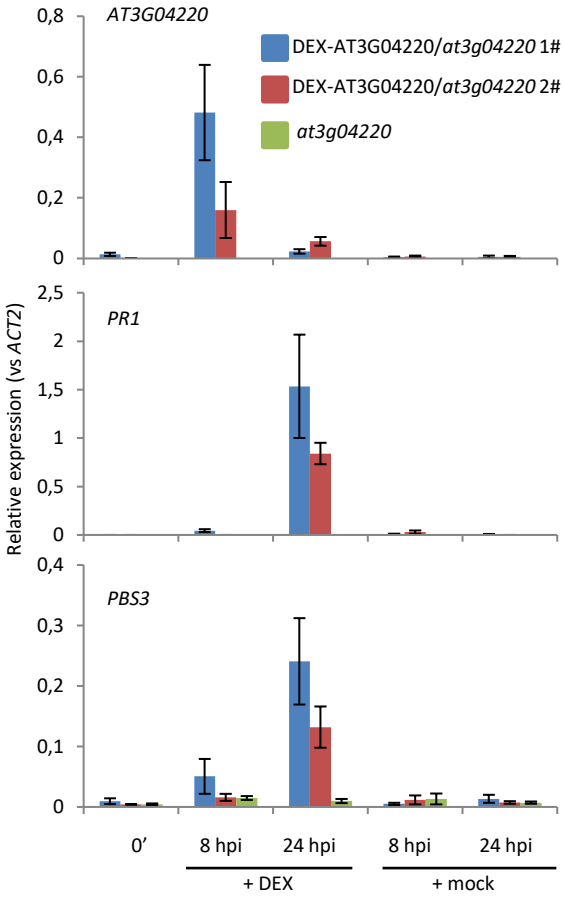


**Figure 8: Upregulation of *AT3G04220* is sufficient to activate the SA sector of defense.** Relative expression levels were measured through RT-qPCR experiments in 2 independent DEX-AT3G04220/*at3g04220* lines and the *at3g04220* line at different time points and in response to dexamethasone (+DEX) or mock. Mean values and SDs were calculated from 3 technical repeats. The experiment was repeated 3 independent times with similar results.

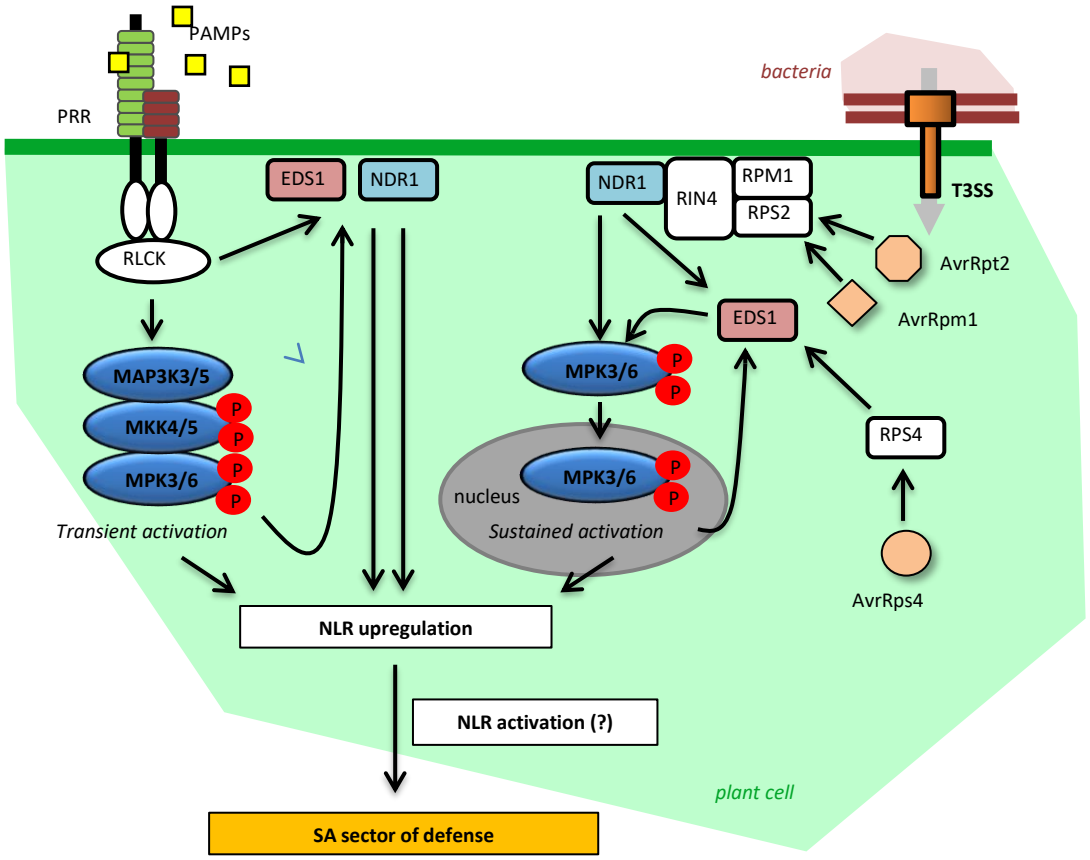


**Figure 9: PTI and ETI responses are intricated around the induction of *NLR* expression in a process involving MPK3/6 activation, and ETI signaling components EDS1 and NDR1.** In PTI context, upon PAMP perception by Pattern-Recognition Receptor (PRR), and signal transduction by Receptor-Like Cytoplasmic Kinases (RLCK), *NLR* upregulation is modulated by transient MPK3/6 activities, NDR1 and EDS1, with the two latters acting downstream or independently of the formers. In ETI context, the effectors AvrRpt2 and AvrRpm1, injected by the bacteria through a Type III Secretory System (T3SS) and targeting RIN4, are recognized by the CNLs RPS2 and RPM1, thereby triggering convergent signaling pathways involving NDR1, EDS1 as well as nuclei-accumulating and sustainably active MPK3/6, to further promote *NLR* expressions. Contrary to what happens in PTI, in ETI, NDR1 and EDS1 act upstream of sustained MPK3/6 activities. The recognition of other effectors, like AvrRps4, can also induce *NLR* expression but to a lesser extent, through the activation of the only EDS1 signaling branch. A positive feedback loop downstream of MPK3/6 and requiring EDS1 contributes to their sustained activation. Finally *NLR* transcriptional upregulation leads to the implementation of the SA sector of defense, through a NLR activation process which remains to be determined.

| Gene | Sequence |
|---|---|
| *AT3G04220* | TGCTGCTGCAACAGGCTTCT |
| | CCCGCGGAAGCTTGGAAAGA |
| *AT3G04220* (for analysis in the *at3g04220* background) | CCTATCGTCTTCATTTCATCTGAG |
| | GACGATTTGATTGGGATGGG |
| *AT4G11170* | TTACCAGAAGAAGGGCTAAG |
| | AACTCCACTCCATAGCTTC |
| *ACT2* | CGTTTCTATGATGCACTTGTGTG |
| | GGGAACAAAAGGAATAAAGAGG |
| *SAND* | AACTCTATGCAGCATTTGATCCACT |
| | TGATTGCATATCTTTATCGCCATC |
| *PR1* | GATCCTCGTGGGAATTATGTG |
| | TTCTCGTAATCTCAGCTCTTATTTG |
| *PBS3* | CGTACCGATCGTGTCATATGAAG |
| | CTTCACATGCTTGGTTATAACTTGC |
| *AvrRpt2* | ACCCGCGCATTACTCGCTAC |
| | CTGCGTTGGCACTTGAACCG |
| *SID2* | AGCTGGAAGTGACCCATCTT |
| | TGGTGAACTGCAAAAACAACA |
| *EDS1* | CTCAATGACCTTGGAGTGAGC |
| | TCTTCCTCTAATGCAGCTTGAA |
| *NDR1* | AGTGGGGTCAAGTAAAGCCG |
| | TCCAACCTGAAAACAGCCGA |
| *CBP60g* | GGTCCAAGATCGAAGCTGAG |
| | TAAATCCCTCAACGGTCCAG |
| *AT1G12290* | TGTGCGAGCATGGGAGTTCA |
| | TCGGGAATGTCAGGGTGGCT |
| *AT5G41750* | AGCAGCAGCCAAGTGGACAA |
| | ACCAAGCTCCCGAAGCCAAC |
| *AT1G66090* | GGAGCCACGCTTTGACCTGT |
| | GCCTCATCGTCCCTGTCTTGG |
| *AT1G15890* | AGTTGAAACACGTGGAAGGACT |
| | TGCATCCAACCCAACTGTGG |
| *AT1G57630* | ACGCAAAGCCTTTCTCAGCCA |
| | AGACAACACCACGAAGAAGCGT |

**Table S1**: List of primers used for qPCR analysis

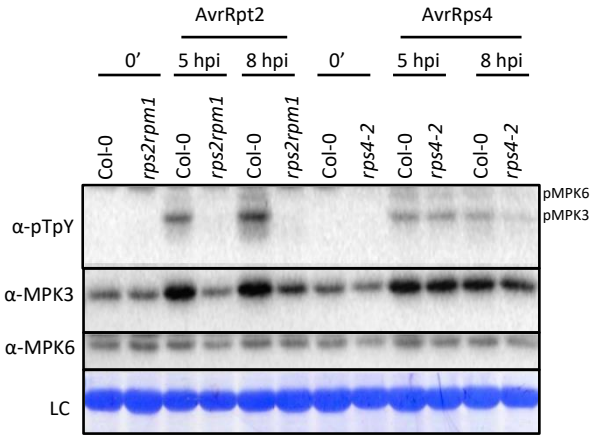


**Figure S1: Sustained MAPK activation is characteristic of RPS2/RPM1-mediated ETI responses.** MPK3/6 activities and quantities were analyzed through immunoblotting with anti-pTpY, anti-MPK3 and anti-MPK6 antibodies in Col-0, *rps2rpm1* and *rps4-2* backgrounds in response to *Pst* AvrRpt2 and AvrRps4. Coomassie staining of blot serves as a loading control (LC). pMPK3 and pMPK6 stand for the phosphorylated and active forms of MPK3 and MPK6. Experiment was repeated at least 3 independent times with similar results.

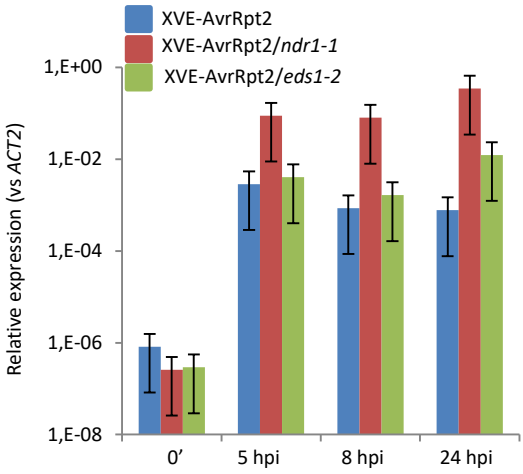


**Figure S2: *AvrRpt2* induction in the XVE-AvrRpt2 lines.** RT-qPCR experiments showing the relative expression levels of *AvrRpt2* in the XVE-AvrRpt2 lines at different times after estradiol treatment. Values with their 90% interval of confidence are represented. Experiment was repeated with similar results for each analysis of the XVE lines.

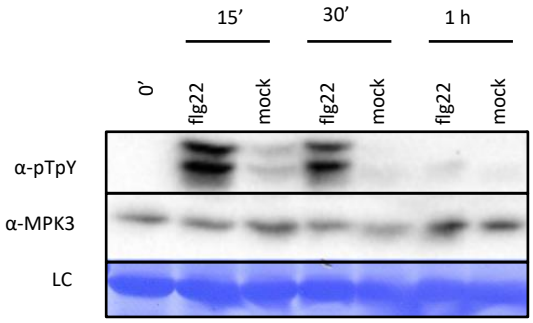


**Figure S3: flg22-mediated vs mock-mediated MPK3/6 activation.** MPK3/6 activities and MPK3 quantities were measured by immunoblotting with anti-pTpY and anti-MPK3 antibodies at different timepoints after flg22 or mock infiltration in Col-0 plants. Coomassie staining of blot serves as a loading control (LC). Experiment was repeated 2 times with similar results.

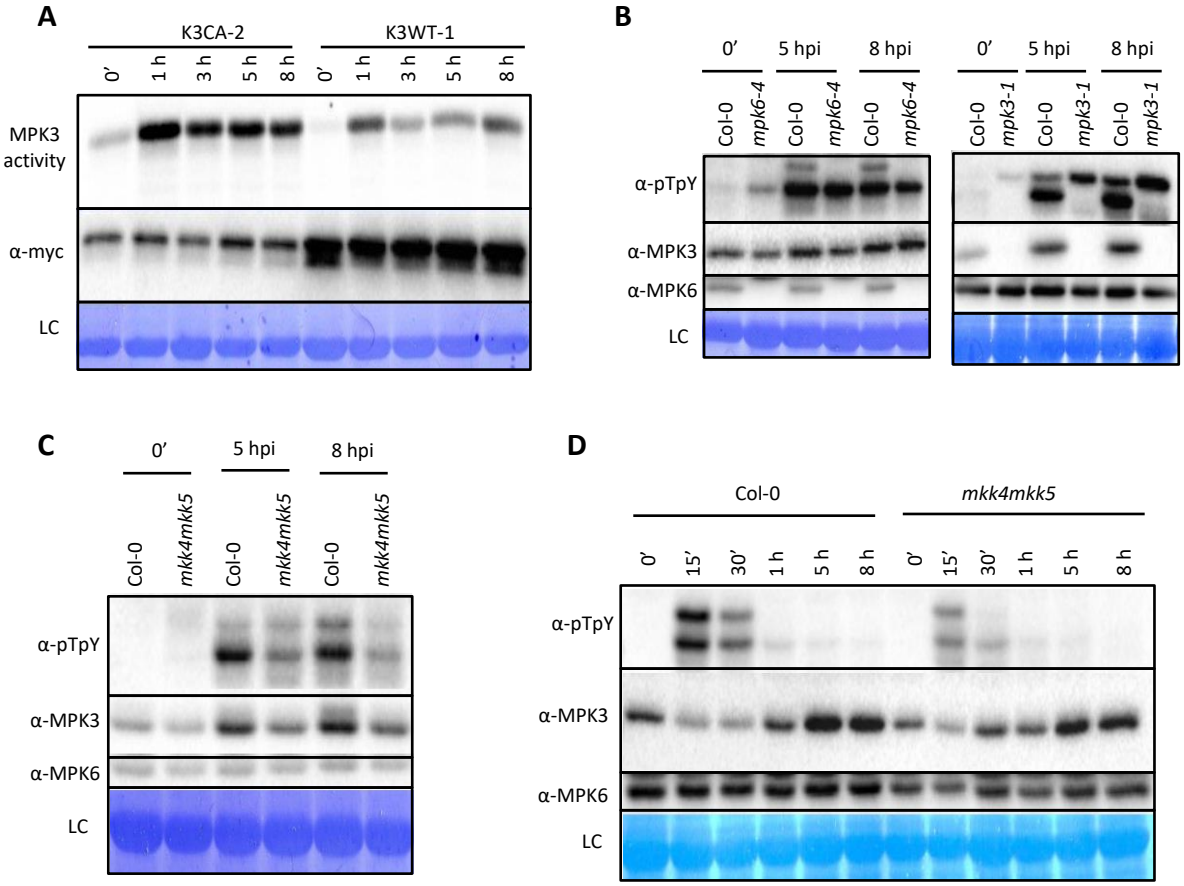


**Figure S4: Misregulation of MPK3/6 activities in K3CA-2, *mpk3-1*, *mpk6-4* and *mkk4mkk5* lines.** (**A**) K3CA activity and quantity at different timepoints after *Pst* AvrRpt2 infiltration were analyzed through an anti-myc immunoprecipitation followed by a kinase assay, and an immunoblotting with anti-myc antibodies. (**B**, **C**, **D**) MPK3/6 activities and quantities were measured by immunoblotting with anti-pTpY, anti-MPK3 and anti-MPK6 antibodies at different timepoints after *Pst* AvrRpt2 infiltration (**B**, **C**) or flg22 treatment (**D**). Coomassie staining of blots serve as loading controls. All experiments were repeated at least 2 times with similar results.

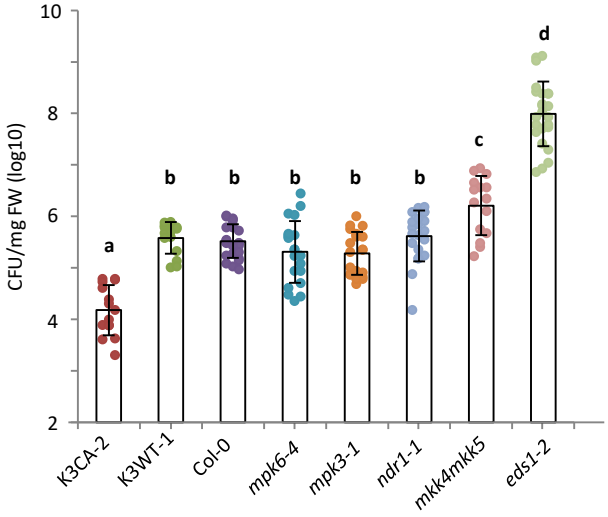


**Figure S5: Resistance phenotypes against the *Pst* AvrRps4 strain.** Plants were infiltrated with same amount of *Pst* AvrRps4 and bacterial load was measured 3 days later. CFU means colony forming unit. Dotplot and histogram showing mean values and SDs for different genotypes were generated from data of at least 3 independent replicates. Letters indicate statistical significance (Kruskall-Wallis test followed by a nonparametric Tukey post-hoc test, $p<0.05$, $15<n<24$).

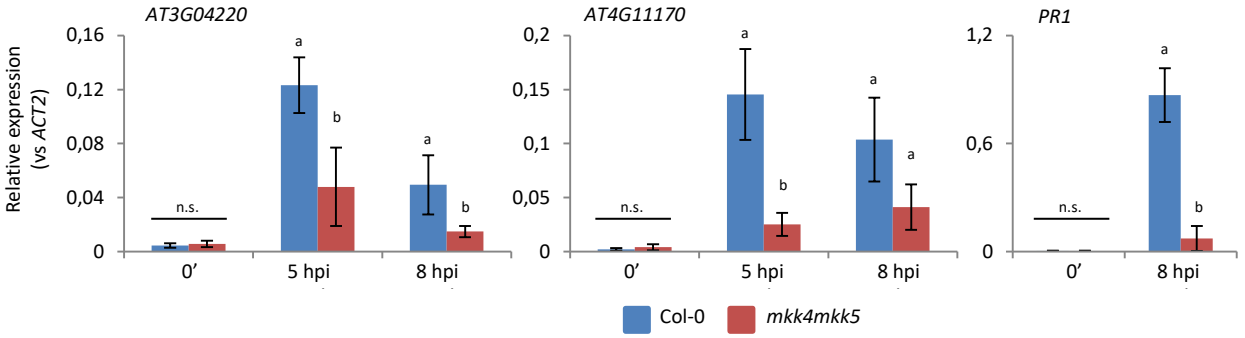


**Figure S6: Upregulation of *AT3G04220*, *AT4G11170* and *PR1* in response to *Pst* AvrRpm1 infiltration in Col-0 and *mkk4mkk5*.** Relative expression levels were measured through RT-qPCR experiments. Mean values and SDs were calculated from 4 technical repeats. Letters indicate statistical differences (Wilcoxon-Mann-Whitney test, $p<0,05$, $n=4$), n.s. stands for not significative. Experiments were repeated 3 independent times with similar results.

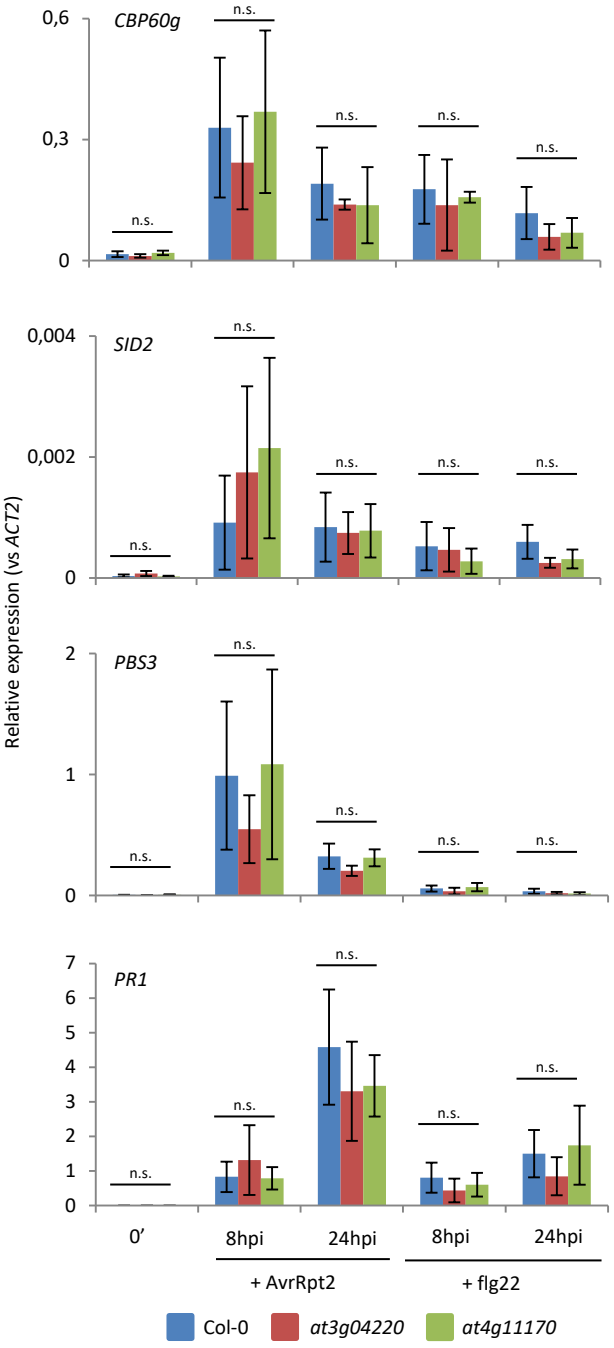


**Figure S7: Expression analysis of the SA sector of defense in Col-0, *at3g04220* and *at4g11170*.** Relative expression levels of *CBP60g*, *SID2*, *PBS3* and *PR1* were measured through RT-qPCR experiments in response to flg22 and *Pst* AvrRpt2. Mean values and SDs were calculated from 4 technical repeats. n.s. stands for not significative (Kruskal-Wallis test, n=4). Experiment was repeated two independent times with similar results.